

A COMPARISON OF TWO METHODS FOR MEASURING
RIGIDITY OF SATURATED MARINE SEDIMENTS

By

James Bryan Lasswell



United States
Naval Postgraduate School



THE SIS

A COMPARISON OF TWO METHODS FOR MEASURING
RIGIDITY OF SATURATED MARINE SEDIMENTS

by

James Bryan Lasswell

December 1970

*This document has been approved for public re-
lease and sale; its distribution is unlimited.*

T137479

11

A Comparison of Two Methods for Measuring
Rigidity of Saturated Marine Sediments

by

James Bryan Lasswell
Lieutenant, United States Navy
B.S., United States Naval Academy, 1963

Submitted in partial fulfillment of the
requirements for the degree of

MASTER OF SCIENCE IN ENGINEERING ACOUSTICS

from the

NAVAL POSTGRADUATE SCHOOL
December 1970

F
L
L
C. 2

ABSTRACT

The results of two different methods for determining the rigidity modulus of a soft sediment are compared. In one method the resonant characteristics of a torsionally oscillating rod which are sensitive to the shear acoustic impedance of the sediment in which the rod is imbedded determine the complex rigidity. The second method utilizes the observation of the phase velocity of an interface wave at the water-sediment boundary. Shear wave speeds computed from the experimental data from both methods are quite similar in magnitude. For the sediment used here, the average value of shear wave speed determined from the interface wave experiment was 33 m/sec while the shear wave speed determined from the measured rigidity was 29 m/sec. The difference lies within experimental uncertainty. Trends in the mass-physical properties of the sediments are investigated by comparing graphically the dependence of both the real and imaginary parts of the complex rigidity on density, porosity, sound speed, silt and clay percentages, Poisson's ratio and density times sound speed squared.

TABLE OF CONTENTS

I.	INTRODUCTION-----	8
II.	EQUIPMENT AND PROCEDURES-----	11
	A. LOCATION OF THE EXPERIMENT-----	11
	B. INTERFACE WAVE MEASUREMENT TECHNIQUE-----	11
	C. THE VISCOELASTOMETER-----	14
	1. Equipment-----	14
	2. Theory and Method of Measurement-----	14
	3. Core Analysis-----	17
	D. COMPRESSIONAL WAVE SPEED MEASUREMENT-----	18
	E. WET DENSITY AND POROSITY-----	19
	F. CALCULATED PARAMETERS-----	19
	G. SAND-SILT-CLAY RATIOS: MINERALOGY-----	20
III.	LIMITATION OF THE METHODS-----	21
	A. RESONANT VISCOELASTOMETER TECHNIQUE-----	21
	B. INTERFACE WAVE TECHNIQUE-----	22
IV.	RESULTS AND DISCUSSION-----	24
V.	CONCLUSIONS AND RECOMMENDATIONS-----	26
	APPENDIX: CLAY MINERALOGY-----	52
	BIBLIOGRAPHY-----	60
	INITIAL DISTRIBUTION LIST-----	62
	FORM DD 1473-----	64

LIST OF TABLES

I.	TABULATED PHYSICAL PROPERTIES-----	27
II.	COMPARISON OF SHEAR SPEED RESULTS-----	31
III.	VARIATION OF CONSTANTS AFTER AVERAGING AT LOW VISCOSITIES-----	32
IV.	CLAY MINERALOGY-----	53

LIST OF FIGURES

1.	Sketch of Interface Wave Measurement Apparatus-----	33
2.	Visicorder Prints From Interface Wave Measurement----	34
3.	Sketch of Viscoelastometer and Associated Equipment--	35
4.	Sketch of Compressional Wave Velocimeter Apparatus---	36
5.	G_1 as a Function of Density-----	37
6.	G_1 as a Function of Porosity-----	38
7.	G_1 as a Function of Sound Speed-----	39
8.	G_1 as a Function of Poisson's Ratio-----	40
9.	G_1 as a Function of Density and Sound Speed Squared--	41
10.	G_1 as a Function of Percent Silt-----	42
11.	G_1 as a Function of Percent Clay-----	43
12.	G_2 as a Function of Density-----	44
13.	G_2 as a Function of Porosity-----	45
14.	G_2 as a Function of Sound Speed-----	46
15.	G_2 as a Function of Poisson's Ratio-----	47
16.	G_2 as a Function of Density and Sound Speed Squared--	48
17.	G_2 as a Function of Percent Silt-----	49
18.	G_2 as a Function of Percent Clay-----	50
19.	Shear Speed as a Function of Sound Speed-----	51
20.	G_1 as a Function of Percent Montmorillonite-----	54
21.	G_1 as a Function of Percent Illite-----	55
22.	G_1 as a Function of Percent Chlorite-----	56

23.	G_2 as a Function of Percent Montmorillonite-----	57
24.	G_2 as a Function of Percent Illite-----	58
25.	G_2 as a Function of Percent Chlorite-----	59

ACKNOWLEDGEMENTS

The author wishes to thank Professor O.B. Wilson, Jr., for his unfailing encouragement and academic counsel. The author also wishes to extend gratitude to the Naval Undersea Research and Development Center, especially to Mr. David Kier for the temporary loan of his Stoneley wave apparatus. Thanks are also due to Dr. R.S. Andrews of the Oceanography Department, Naval Postgraduate School for his advice on some of the field techniques, for arranging the mineralogy analyses and to Ensign W. Walsh for providing the size analyses of our samples. Thanks also to Mr. K. Smith for his electronic wisdom and patient assistance. Special thanks are due to my wife and children who suffered with my impatient moods during the completion of this project. Financial support was received from the Foundation Research Program of the Naval Postgraduate School.

I. INTRODUCTION

Growing concern for the accurate and comprehensive description of the acoustic reflection and attenuation characteristics of the ocean bottom is continually stimulated by attempts to fill the large gap in predictability of the actual reflection losses. The development of a model for the reflection coefficient which more accurately describes the physics of transmission and reflection should result in improved capability for predicting transmission loss for sound in the ocean in those cases where bottom interaction is important, such as passive and active sonars in shallow water and active sonars using the bottom bounce mode.

Historically, the ocean bottom has most often been modeled as an interface between two fluids of differing densities and sound speeds. Usually referred to as the Rayleigh model, it is generally accepted because normal surficial sediments have high porosities and low rigidities which approximate those of a fluid. The Rayleigh model is sometimes found to be deficient, especially at lower grazing angles [3,9].

Some have accounted for this disparity by presuming that the sediment possesses a finite rigidity and hence is capable of supporting a shear wave [3]. Using a viscoelastic model and complex Lamé constants, one is capable of describing the formation of shear-interface waves and absorption of compressive sound waves in the sediment. Bucker, et al. [3] finds better agreement with

experimental measurements for the theoretically calculated bottom loss using this viscoelastic model and associated sediment parameters obtained by Hamilton [9,10,11] than for the Rayleigh model in a number of cases.

In order to obtain both complex Lamé' constants for the viscoelastic model it is required that, in addition to the measurement of sound absorption, both shear wave speed and compressional wave speed be measured. Hutchins [12] demonstrated the feasibility of measuring the complex shear modulus of soft sediments (artificial) by noting the effects caused by the rigidity on the resonant behavior of a torsionally oscillating rod imbedded in the sediment. Utilizing a laboratory prepared kaolin-water mixture, he developed the viscoelastometer technique in the frequency range of 38.3 to 38.9 KHz.

Cohen [5], by improving the design of the instrument, increased the range of operation to 5.8 to 38 KHz. Cohen used both kaolin-water and bentonite-water combinations as artificial sediments.

Utilizing Hutchins' and Cohen's observations that soft, clayey, simulated sediments did, in fact, have a measureable shear modulus, Bieda [2] continued this research by developing a new viscoelastometer suitable for use in making in situ measurements and the subsequent laboratory analysis of 20 sediment cores obtained in the Monterey Bay area.

The results obtained from use of these probes [2,5,12] are quite encouraging and are certainly within reasonable bounds for

this type of sedimentary material (E.L. Hamilton, personal communication). However, there has been no independent determination of the rigidity for comparison and verification of the method. Consequently it was required that experiments be conducted that would test the validity of the probe method. Successful development of such a probe would make the necessary measurements of ocean bottom parameters a more convenient operation.

Another method for determining the elastic constants involves measuring directly both the compressional wave and shear wave speeds; knowing these, it is a simple matter to determine the real elastic constants. The imaginary parts of the elastic moduli must be obtained from measurements of the attenuation of the compressional and shear waves. The former method is used in this experiment as an independent means for validating the measurement of the real components of the rigidity made by the viscoelastometer developed by Bieda [2]. The method described is essentially the same as that used by Hamilton, et al. [11] in measurement of the interface wave speed and compressional wave attenuation in sediments in the San Diego area¹.

¹Some controversy appears to exist as to just what title should be applied to the interface wave that exists at the surface between an elastic, solid bottom and the overlying water. Although generally referred to as Stoneley waves, it appears that Stoneley [17] never included the possibility that the upper medium could be a fluid. Other people tend to choose the name Scholte waves since Scholte [16] generalized the nomenclature to include fluid-solid interface waves. Since the environment in which the author's data were taken did not entirely approach an elastic-solid bottom of infinite extent below a infinite half-space of homogeneous fluid, it was decided to use the term "interface wave" when describing the elastic wave existing at the interface between the bottom and the overlying water.

II. EQUIPMENT AND PROCEDURES

A. LOCATION OF THE EXPERIMENT

Cohen [5] has shown the viscoelastometer to be ineffective in sediments of large mean grain size, possibly because the grain dimension becomes comparable to the shear wavelength in the sandy sediments and therefore the assumption of homogeneity becomes invalid. Thus there was a need for finding a sediment which was silty clay or clayey silt.

There are vast areas of mud bottoms in the Monterey Submarine Canyon area of Monterey Bay, California, that would normally suffice for this type of experiment. However, since the services of a submersible platform were not available the evaluation had to be made at a quite shallow depths (1 to 1.5 m) near shore. A suitable mud sediment site was found in the tidal flats of the Kirby Park area of Elkhorn Slough, a few miles north of the city of Monterey.

B. INTERFACE WAVE MEASUREMENT TECHNIQUE

Direct measurement of the speed of shear waves in very soft marine sediments is made virtually impossible at acoustic frequencies because of the rapid attenuation of the shear waves and the difficulty of coupling a suitable transducer to the medium. It has, however, been determined by Strict and Ginzburg [18] and by Hamilton, et al. [11] that the ratio of the shear wave speed

to the interface wave speed remains relatively constant for a given value of the ratio of the two densities of adjoining media irrespective of other varying bottom constants.

While compressional wave speed and wet density of the sediment can easily be measured in the laboratory and corrected to in situ values, it was required that the interface wave speed be measured and corrected to shear speed as previously accomplished by Hamilton, et al. [11].

An interface wave, generated by the detonation of a blasting cap at the water-sediment interface, is examined using three or four vertically-polarized, velocity-sensitive geophones mounted at known intervals on the interface. An aluminum rod and flexible lines served as a convenient support and the means for spacing of the geophones and the electrically-fired blasting caps which were mounted under a heavy brass plate.

During the firing of these blasting caps, the response of the geophones is monitored at a remote station. The signal from the geophones passes through an impedance-matching transformer, a set of attenuator pads and a low-noise amplifier capable of as much as 50 db gain to a Honeywell Visicorder where the subsequent amplitude versus time responses are plotted as shown in Figure 2. A sketch of the operational assembly is shown in Figure 1.

The Visicorder traces are studied to determine the points of constant phase in each of the geophone traces (point a in Figure 2). This is generally best accomplished by attempting to match waveforms

which is somewhat aided by irregular spacing of the geophones and adjustment of gain so that amplitudes are comparable. Having found the points of constant phase, and using convenient time reference marks, the interface wave speed is easily determined.

Having obtained the interface wave speed, the graphs provided by Strict and Ginzburg [18] are entered with the ratio of the density of the overlying sea-water to the density of the sediment. The graphs are plotted with the ratio of interface wave speed to shear wave speed versus the ratio of shear wave speed to compressional wave speed, varying the parameter ratio of water density to sediment density. Since both the ordinate and abscissa are ratios involving the unknown, shear wave speed, an additional assumption about the magnitude of shear wave speed allows one to accurately determine the necessary value. As the ratio of shear wave speed to compressional wave speed approaches 0.5, the individual graphs all begin to approach a horizontal asymptote which may conveniently be read from the ordinate with a maximum possible error of 5 percent.

Having determined the value of the ratio of the interface wave speed to shear wave speed, and knowing the interface wave speed, it is easy to compute the shear wave speed ($V_s = V_i/A$, where A is the ratio, V_s the shear wave speed and V_i the interface wave speed).

C. THE VISCOELASTOMETER

1. Equipment

The apparatus designed by Bieda [2] is a result of a series of improvements on the original devices constructed and evaluated by Cohen [5] and Hutchins [12]. It consists of a $10\frac{1}{2}$ -inch long, $\frac{1}{2}$ -inch diameter cylindrical rod which is excited in torsional oscillation by a centrally mounted barium titanate transducer. The rods, constructed from a constant modulus alloy, NI-Span-C, were heat-treated and highly polished. The electrical leads to the transducer are passed through a supporting yoke which supports a clamp that holds the transducer in position. The clamp is secured to the transducer at its center, a node of torsional motion for all resonant modes in the rod. A sketch of the apparatus is shown in Figure 3. Various compounds were used to maintain the water-tight integrity of the electrical connections, generally RTV insulating rubber was deposited in the large crevices at the junction of the clamp and the transducer while the other boundaries were coated with varnish or glyptol.

A Dranetz 100B Impedance-Admittance meter, a suitable oscillator and a frequency counter were used to measure the electrical conductance and the resonant frequencies.

2. Theory and Method of Measurement

When the viscoelastometer is excited at its mechanical resonance, a torsionally oscillating standing wave exists along the axis of the rods and transducer. The torsional motion of the walls of the rod generates a shear wave which propagates radially

outward into the sediment. The radiation impedance of the surrounding sediment has a modifying effect on the magnitude of the electrical resistance of the probe and its frequency of mechanical resonance, compared to those values measured in air (approximately no-load conditions). The change in resistance and resonant frequency are thus direct functions of the rigidity of the sediment [14].

Under the assumption that the shear waves that propagate outward from the viscoelastometer have wavelengths much smaller than the radius of curvature of the rods and that the amplitude of these shear waves is very rapidly attenuated, the waves propagated in the sediment may be considered to be plane waves with the formula:

$$T = T_0 \exp [\sqrt{\pi f \rho / \eta} (1+i) z] \quad (1)$$

where T is the shear stress amplitude, T_0 the initial amplitude, f the frequency, and η the shear viscosity. The harmonic time-varying function has been suppressed for sake of convenience.

In a Newtonian fluid, the coefficient of shear viscosity is $\eta = T/\dot{S}$, where S is the shear strain and $\dot{S} = \partial S/\partial t$. In our viscosity model a complex rigidity (G_c) has been assumed along with a complex viscosity (η_c). Thus,

$$\eta_c = \eta_1 - i\eta_2 \text{ and } G_c = G_1 + iG_2. \quad (2)$$

In a Newtonian fluid, $\eta_2 = 0$, and $\eta_1 = 0$ in a perfectly elastic solid. Since $\eta_c = T/i\omega S = -iG_c/\omega$ for simple harmonic motion, where ω is the angular velocity,

$$G_1 = \omega\eta_2 \text{ and } G_2 = \omega\eta_1. \quad (3)$$

The specific radiation impedance (Z) of the sediment is the ratio of shear stress to particle velocity. Following Mason [14] and McSkimin [15], for a Newtonian fluid

$$Z = R + iX = \sqrt{\pi f \eta \rho} (1 + i) \quad (4)$$

where R and X are the specific acoustic impedance and reactance of the sediment, respectively, and ρ is the sediment density. For the case when viscosity is complex, the following relations result:

$$\begin{aligned} \eta_1 &= \frac{2RX}{\omega \rho} & \eta_2 &= \frac{R^2 - X^2}{\omega \rho} \\ G_1 &= \frac{R^2 - X^2}{\rho} & G_2 &= \frac{2RX}{\rho} \end{aligned} \quad (5)$$

Thus, it becomes apparent that determination of the complex rigidity or viscosity requires only a knowledge of real and imaginary parts of the specific acoustic impedance for plane shear waves.

Mason [14] has shown that constants of proportionality can be determined which relate the total acoustic resistance² (R_t) to the change of electrical resistance (ΔR_e), i.e., $\Delta R_e = K_1 R_t$, and the total acoustic reactance (X_t) to the change of resonant frequency (Δf), i.e., $\Delta f = K_2 X_t$, when the loading on the rod is changed from air to the medium under study. Here, $R = R_t/l$ and $X = X_t/l$, where l is the length of the probe immersed in the sediment. Thus, measurement of the acoustic impedance is reduced

²Transducer which drives the rod.

to measurement of the change observed in the frequency of resonance and in the resonant value of electrical conductance when the probe is operated in the material to be analyzed.

Evaluation of the constants K_1 and K_2 is accomplished by measurement of ΔR_e and Δf in Newtonian calibration fluids. Since $\eta_2 = 0$ in a Newtonian fluid, $R = X$; knowing the viscosity and density of the test fluid, the procedure for calculating K_1 and K_2 is straightforward.

3. Core Analysis

In the same relative location of the interface wave experiment ten cores were taken for purposes of viscoelastometer analysis, density and compressional wave speed measurement. While maintaining the core at its original temperature, the complex rigidity is determined using Bieda's equipment. The measured real part of rigidity and the observed density are used to determine a shear wave speed, i.e., $V_s = (G_1/\rho)^{\frac{1}{2}}$.

The core samples were analyzed at two of the resonant frequencies, 27 kHz and 38 kHz, due to anomalous behavior at the lower frequencies, especially in the stiffer samples. Since the constants K_1 and K_2 tend to vary with frequency and viscosity, an average value was used at each frequency from calibrations in fluids with viscosities roughly equivalent to those expected in the sediments. Table III contains examples of the variance of these constants over temperature and viscosity.

The computed shear velocities are averaged and are compared to the value for shear velocity obtained in the interface wave experiment in Table II.

D. COMPRESSSIONAL WAVE SPEED MEASUREMENT

Compresssional wave speed is measured in each of the sample cores by determination of the time required for a 2 MHz compresssional pulse to pass through a known length of sediment. Barium titanate disk transducers are used as a transmitter and as a receiver, while the transmitted pulse width and frequency are varied in close proximity to 2 MHz in order to obtain resonant operation of the transducers.

The two transducers are mounted facing each other as shown in Figure 4. The sample, approximately 3 inches long, is inserted in the holder which is in contact with one transducer; the other transducer can then be moved to contact the other end of the sample. A dial indicator is used to measure the separation while a time mark generator and the output of a triggered pulsed oscillator are displayed on the face of a dual trace oscilloscope. The temperature is maintained at a constant value, identical to that measured during the interface wave experiment.

Calibration of the velocimeter is accomplished by measuring a sequence of time delays for various transducer spacings in a mixture of 22 parts ethanol to 100 parts distilled water. This combination was shown to be relatively insensitive to small temperature changes in the neighborhood of the temperatures of this experiment [21].

The sediment sound speeds and the speed of sound in the water samples (computed using Wilson's equation) taken in the vicinity of the experiments are shown in Table I.

E. WET DENSITY AND POROSITY

Wet density is measured by weighing a known volume of the saturated sediment. The weight of this same sample after heating in an oven at 105°C for a period of 24 hours is again determined. If it is assumed that the weight lost is completely derived from evaporation of the entrapped water and that the weight of 1 ml of water is 1g, the porosity (P) is easily calculated,

$$P = \frac{\text{Volume of Voids}}{\text{Total Volume}} \quad (6)$$

F. CALCULATED PARAMETERS

The shear wave speed is calculated by use of the real part of the measured rigidity, G_1 , and the sediment density, ρ , in the formula:

$$v_s = \sqrt{\frac{G_1}{\rho}} \quad ; \quad (7)$$

shear wave speed is also computed from interface wave speed by the formula:

$$v_s = v_i/A \quad , \quad (8)$$

where A is the constant of proportionality derived from the graphs of Strict and Ginzburg [18]. Poisson's ratio σ , is calculated by the relation:

$$\sigma = \frac{1}{2} \left[1 - \frac{1}{((v_p/v_s)^2 - 1)} \right] \quad (9)$$

where V_p is the compressional wave speed and V_s is the shear wave speed. The measured and computed physical constants are shown in Table I.

G. SAND-SILT-CLAY RATIOS: MINERALOGY

Sand-silt-clay ratios were calculated at the Naval Postgraduate School by the sieve pipette method. Clay mineralogy analyses, performed by Dr. W.R. Bryant, Texas A&M University, are shown in the Appendix.

III. LIMITATION OF THE METHODS

A. RESONANT VISCOELASTOMETER TECHNIQUE

While usage of this probe is not strictly limited to the laboratory, a very strong dependence on temperature of the constants K_1 and K_2 (Table III) requires that measurements for comparison be made in a temperature-controlled environment. To allow for correct measurements to be made from 2-3/4 inch diameter cores, the assumption is made that the shear wave length is much smaller than the distance from the probe to the core liner. It was noted that at the lower frequency, especially in stiffer sediments, erratic readings were generally obtained, possibly from the violation of this assumption. This limitation should not pose any great problems when the probe is used in situ as there should then be no surrounding barrier in coupling to the motion of the oscillating rods.

It was also noted that the values of K_1 and K_2 vary with changing viscosity as well as frequency and temperature. Consequently, the final constants used were obtained from an average of those values obtained over the lower values of viscosity (1-15 poise). This could cause an error in K_1 of no more than 30 percent and perhaps 110 percent in the value of K_2 .

Another obvious limitation to the laboratory analysis is that no matter how carefully a core is taken, there is always some structural distortion of the sample as well as some drying before analysis can be made.

B. INTERFACE WAVE TECHNIQUE

The most serious breach of assumptions occurs in the measurement of the interface waves at shallow depths. The determination of the interface wave speeds are all predicted on an interface between liquid and elastic-solid half spaces [4,7]. In the measurement of the lower frequency (about 10 Hz) interface waves in shallow water it would seem that the effect of the overlying water is quite small, since the wavelength for 10 Hz compressional waves in water is so large compared to the depth. Thus, the situation is very nearly that normally encountered for Rayleigh waves. This effect could cause the ratio of the interface wave speed to the shear wave speed, A , to approach a value of 0.92 [4]. This could yield a possible error in the measured shear wave speed of as much as 10 percent.

Higher frequency compressional waves, although much faster, occasionally tend to mask the arrival of the interface wave due to the exponential tail of the explosion. Often this masking caused some uncertainty as to the actual arrival time of the interface wave. The standard deviation of the measured values of interface wave speed are about 11 percent of the average measured value.

Since the distance between the geophones enters directly into the computation of the interface wave speed, the uncertainty of about 2 cm could yield an error of about 5 percent in the result.

Since only quantitative information describing the relationship between interface wave and a solid shear wave is that given by Strict and Ginzburg [18], the author was forced to make

the approximation that shear wave speed would always be less than one-half the compressional wave speed in order to obtain a value for the needed ratio, A, as noted in section II-B. This uncertainty in the constant, A, could yield an error of no greater magnitude than 5 percent.

IV. RESULTS AND DISCUSSION

Table II presents a comparison of the two methods of measuring rigidity by showing the average values of the shear wave speed as calculated from measurements of the real part of the rigidity and the shear wave speed computed from the interface wave experiment. Extremely good correlation between the two values tends to confirm the validity of the torsional viscoelastometer results. It must be pointed out, however, that the viscoelastometer was operated at frequencies of 27 kHz and 38 kHz while the interface wave frequencies were about 10 Hz. Although there is a great disparity in frequencies, there is no reason to expect that dispersion of shear speed should occur [11]. The viscoelastometer technique is subject to a maximum precision of 30 percent in calculating the real part of the rigidity, largely arising from an inability to accurately measure all the parameters. While these uncertainties of the method point toward the need for stricter maintenance of conditions during viscoelastometer measurements and during calibration, they are not of sufficient magnitude to discredit the method.

The mechanical disturbance in coring and in transporting the samples very likely disturbs the physical properties by an indeterminate amount. It is also known from a visual inspection of the cores that the bottom in this area was far from being homogeneous, in either the horizontal or the vertical plane.

The measured physical parameters for the ten cores taken tend to follow the same general patterns (Figures 5 to 19) as did those presented by Bieda [2] with the major exception that the cores taken in the slough possess less than 7 percent sand, making them much more acceptable for viscoelastometer analysis.

It is significant to note that the rigidities obtained ranged between 5.1×10^6 to 2.7×10^6 dynes/cm² for the real part and 1.1×10^6 to 7.9×10^6 dynes/cm² for the imaginary part. These values, as pointed out by Bieda [2], are significantly lower than those found by Hamilton [11], but additional evidence continues to point toward the direction of lower rigidities in surficial sediments [1,6].

The trends noted by Bieda were also observed in this research; the real part of rigidity increases with increasing density, increasing percent silt and with increasing ρV_p^2 . Rigidity decreases with increasing porosity and percent clay. The same trends are noticeable but less marked with the imaginary part due to the greater degree of scatter caused by experimental imprecision.

V. CONCLUSIONS AND RECOMMENDATIONS

The relatively close agreement of the two values of shear wave speed strongly tends to validate the usefulness of the viscoelastometer technique for measuring the real part of the complex rigidity in soft, fine grained surficial marine sediments.

The mass-physical trends noted by Bieda [2] are seemingly substantiated by these observations but require a great deal more study to completely classify definite behavioral functions.

In order to further exploit the use of the viscoelastometer, it is recommended that further efforts be applied to the design of the viscoelastometer in order to minimize the effects on its calibration of grain size, stiffness and temperature.

Further effort is also indicated toward improving the precision in measuring the imaginary part of the complex rigidity and toward its validation, utilizing a measurement of the sound absorption in the sediment as a test.

Construction of an artificially prepared ocean bottom (kaolin-water) is recommended in order to circumvent the damage done to the cores when taken from the bottom and to improve homogeneity and temperature stability of the medium.

TABLE I. Tabulated Physical Properties

<u>SAMPLE</u>	<u>SOUND SPEED</u> m/sec	<u>SHEAR SPEED</u> m/sec	* <u>CSED/ CWAT</u>	<u>POISSON'S RATIO</u>
1.	1487.0	22.1	0.983	0.499 ₈₉
2.	1502.0	21.5	0.993	0.499 ₈₉
3.	*****	32.9	*****	*****
4.	1510.0	21.1	0.998	0.499 ₉₀
5.	1505.5	23.5	0.995	0.499 ₈₇
6.	1506.1	26.4	0.995	0.499 ₈₄
7.	1517.3	47.0	1.000	0.499 ₅₁
8.	1510.1	33.5	0.998	0.499 ₇₅
9.	1493.8	33.1	0.987	0.499 ₇₅
10.	1520.1	28.8	1.000	0.499 ₈₂

***** Sound speed unattainable

* Compressional speed in sediment/compressional speed in water

TABLE I. Tabulated Physical Properties (cont.)

<u>SAMPLE</u>	$\frac{G-1}{10^6}$ dynes/cm ²	$\frac{G-2}{10^6}$ dynes/cm ²	<u>DENSITY</u> g/cm ²	<u>POROSITY</u> %
1.	5.8	2.5	1.21	65.9
2.	5.1	3.0	1.25	64.7
3.	14.8	6.9	1.35	74.4
4.	6.0	1.8	1.36	78.3
5.	7.6	1.1	1.37	72.9
6.	9.8	2.7	1.40	74.4
7.	27.8	7.9	1.25	72.5
8.	17.3	7.0	1.54	68.9
9.	16.1	5.2	1.46	71.1
10.	12.2	5.8	1.47	72.0

TABLE I. Tabulated Physical Properties (cont.)

<u>SAMPLE NUMBER</u>	<u>PERCENT SAND</u>	<u>PERCENT SILT</u>	<u>PERCENT CLAY</u>
1.	2.8%	29.4%	67.8%
2.	7.2%	52.6%	40.4%
3.	2.2%	70.9%	26.9%
4.	6.5%	25.7%	67.8%
5.	1.4%	56.5%	42.1%
6.	1.9%	70.8%	27.3%
7.	2.0%	72.2%	25.8%
8.	1.9%	79.6%	18.5%
9.	2.2%	79.7%	18.1%
10.	2.2%	72.3%	25.5%

TABLE I. Tabulated Physical Properties (cont.)

<u>SAMPLE</u>	$(10^6 \frac{\rho C^2}{\text{g-m}^2/\text{cm}^3\text{-sec}^2})$
1.	2.67
2.	2.82
3.	****
4.	3.67
5.	3.10
6.	3.17
7.	2.87
8.	3.52
9.	3.26
10.	3.40

**** Sound speed unattainable

TABLE II. Comparison of Shear Speed Results

	<u>AVERAGE VALUE</u>	<u>STANDARD DEVIATION OF DATA POINTS</u>	<u>ESTIMATE OF PRECISION</u>
Ratio of V_i/V_s	0.758	0.062	<u>+ 5 %</u>
Shear wave speed (from measured rigidities)	29.0 m/sec	8 m/sec	<u>+ 30%</u>
Interface wave speed (from interface wave experiment)	28.8 m/sec	4 m/sec	<u>+ 10%</u>
Shear wave speed (from above)	33.3 m/sec	4 m/sec	<u>+ 15%</u>

TABLE III.

Variation of Constants After Averaging at Low Viscosities

<u>Temperature (°C)</u>	<u>K₁</u>		
	<u>4kHz</u>	<u>27 kHz</u>	<u>38 kHz</u>
10	6.04	0.43	0.34
17	5.73	0.69	0.62
22	6.20	0.71	0.70

<u>Temperature (°C)</u>	<u>K₂ (K₂ x 10⁻³)</u>		
	<u>4kHz</u>	<u>27 kHz</u>	<u>38 kHz</u>
10	1.36	1.38	1.52
17	2.96	2.67	2.83
22	3.81	2.66	2.72

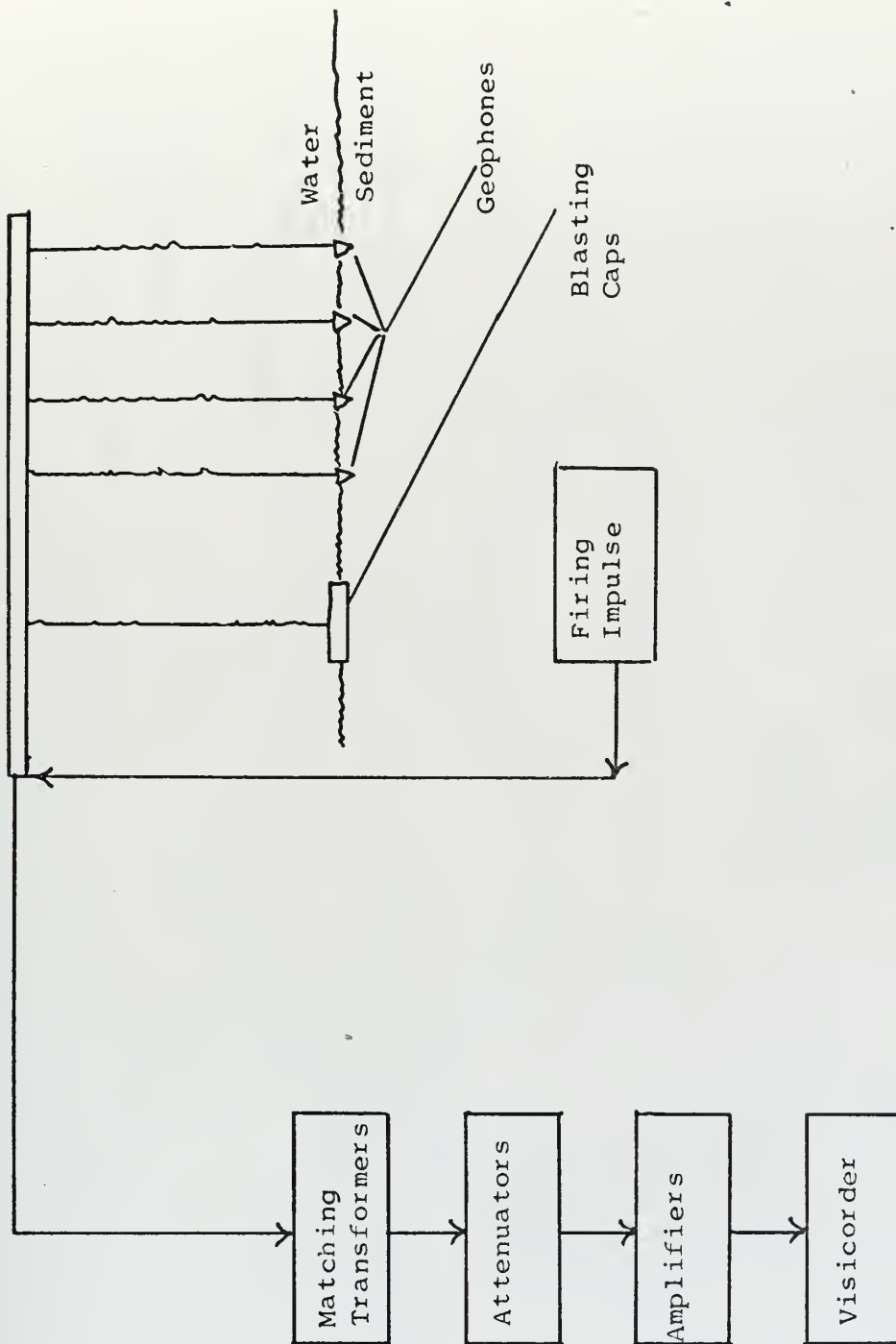


Figure 1. Sketch of Interface Wave Measurement Apparatus

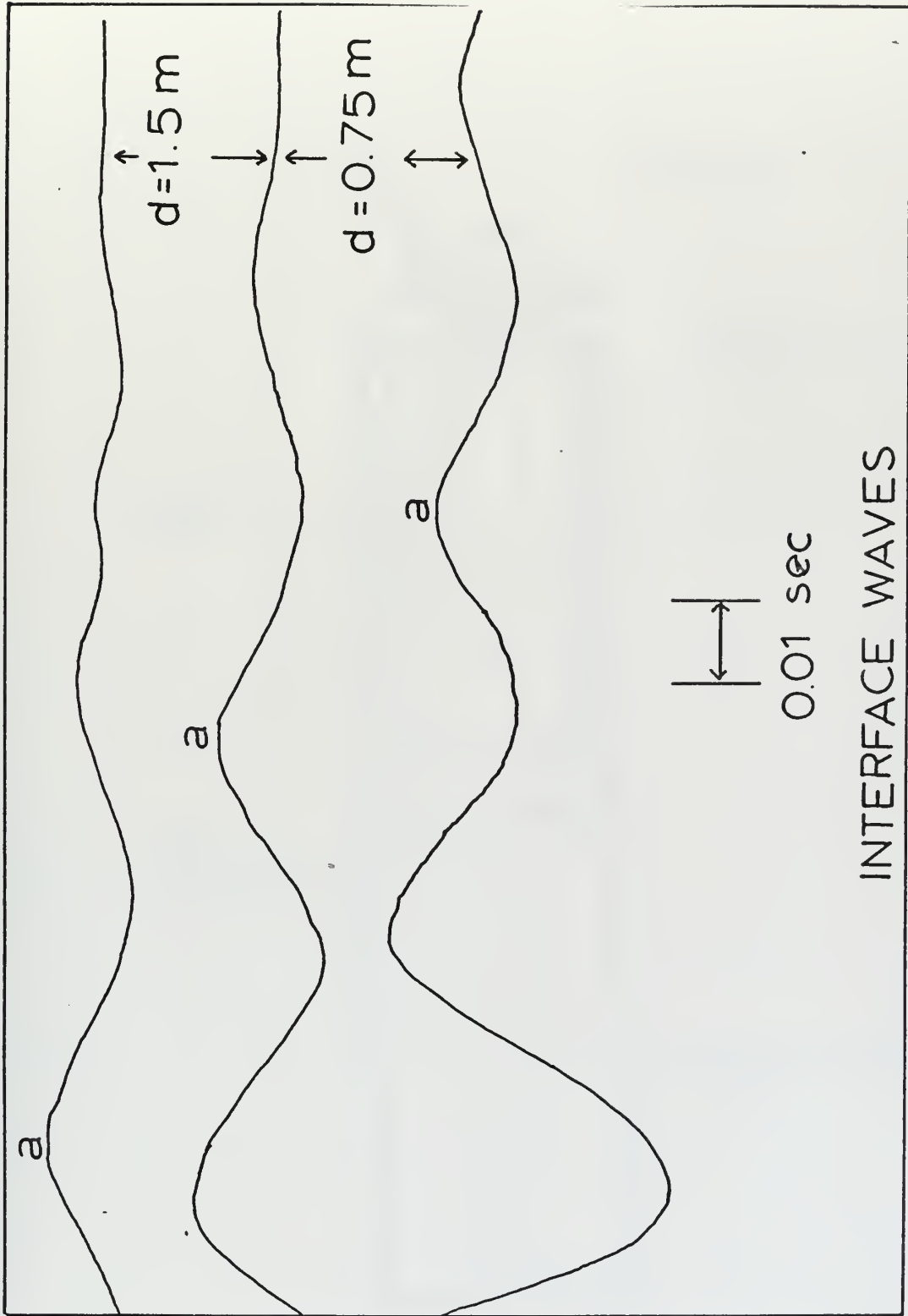


Figure 2. Visicorder Prints from Interface Wave Measurement

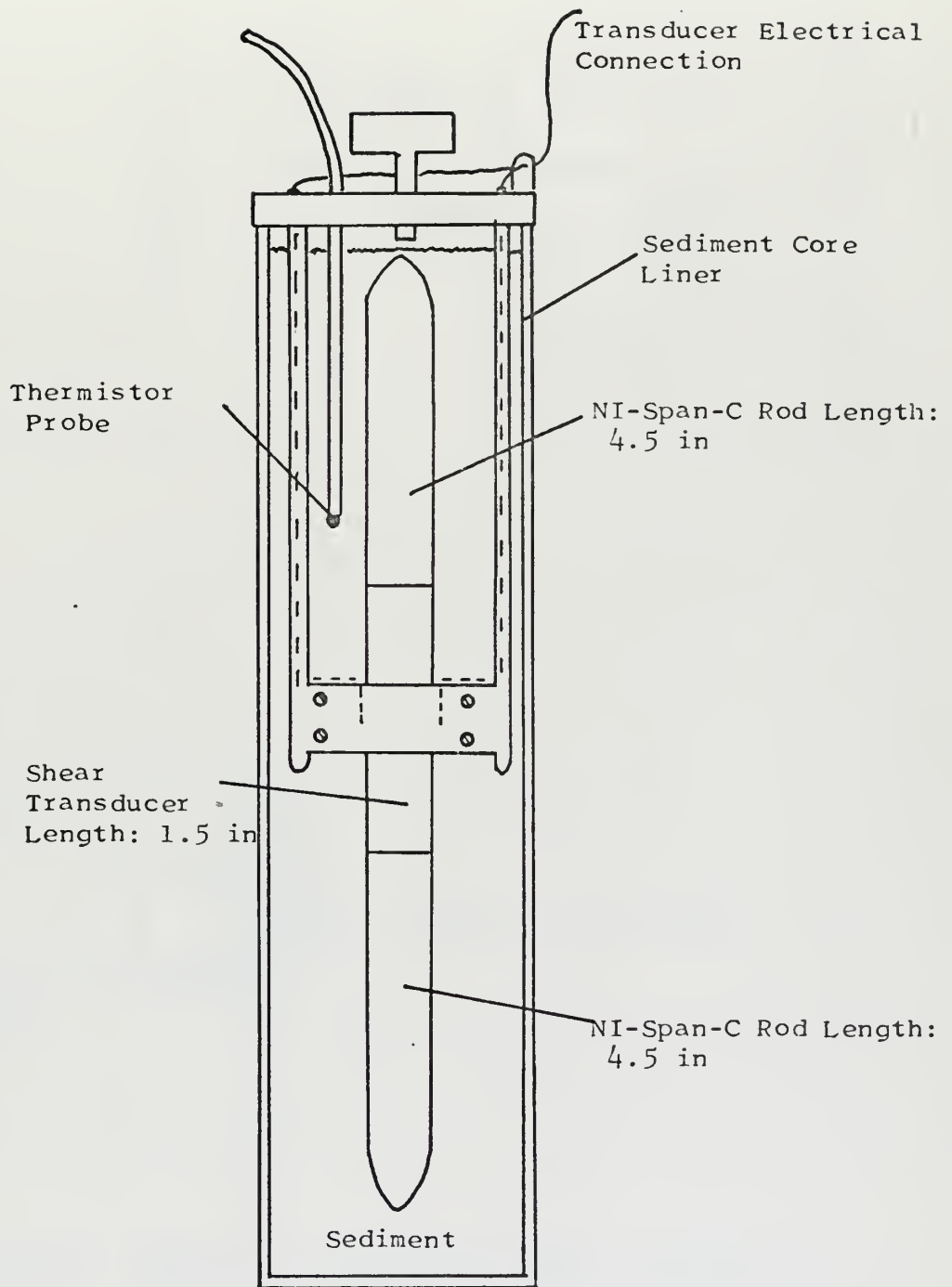


Figure 3. Sketch of Viscoelastometer and Associated Equipment [2]

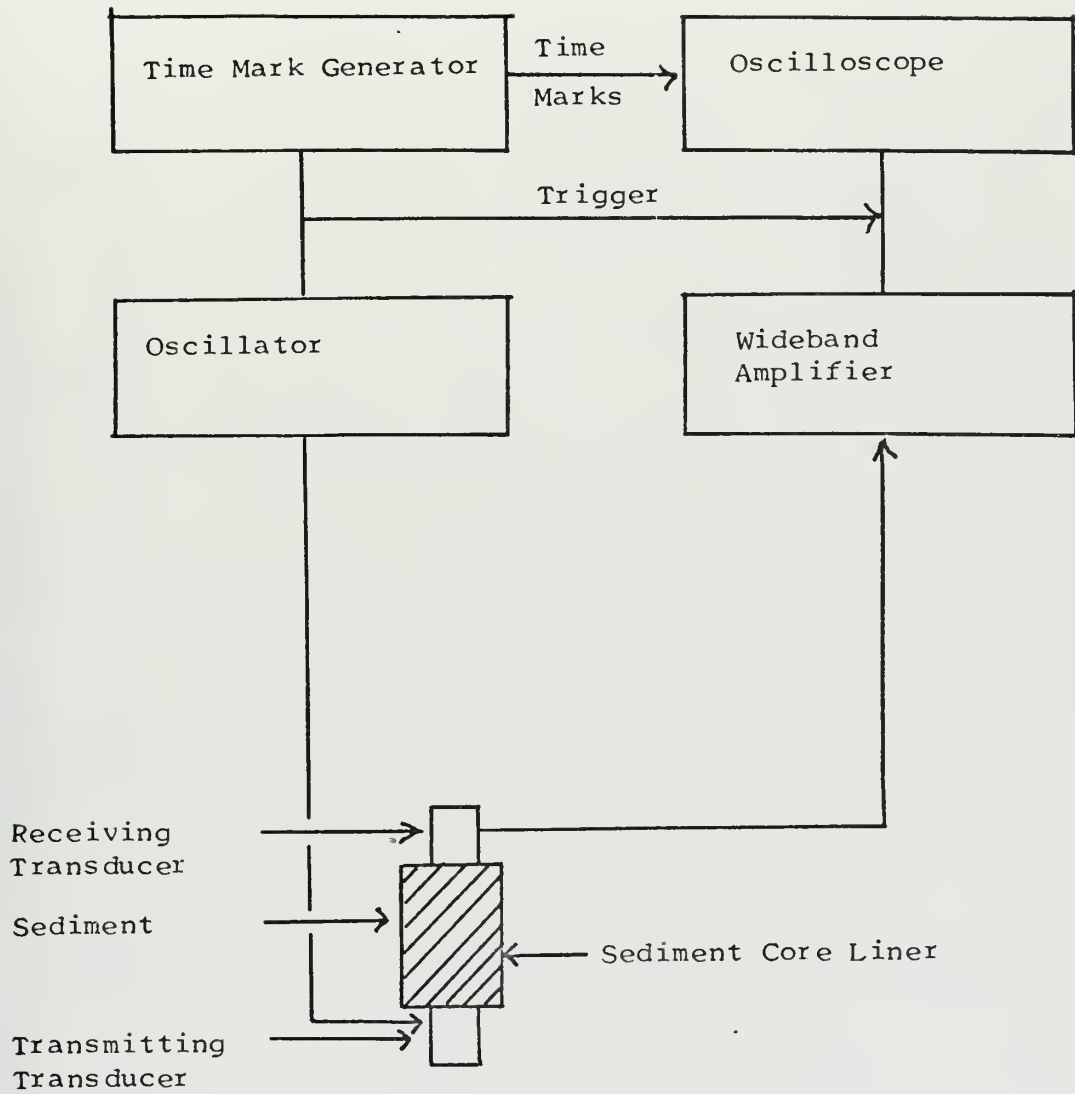


Figure 4. Sketch of Compressional Wave Velocimeter Apparatus [2]

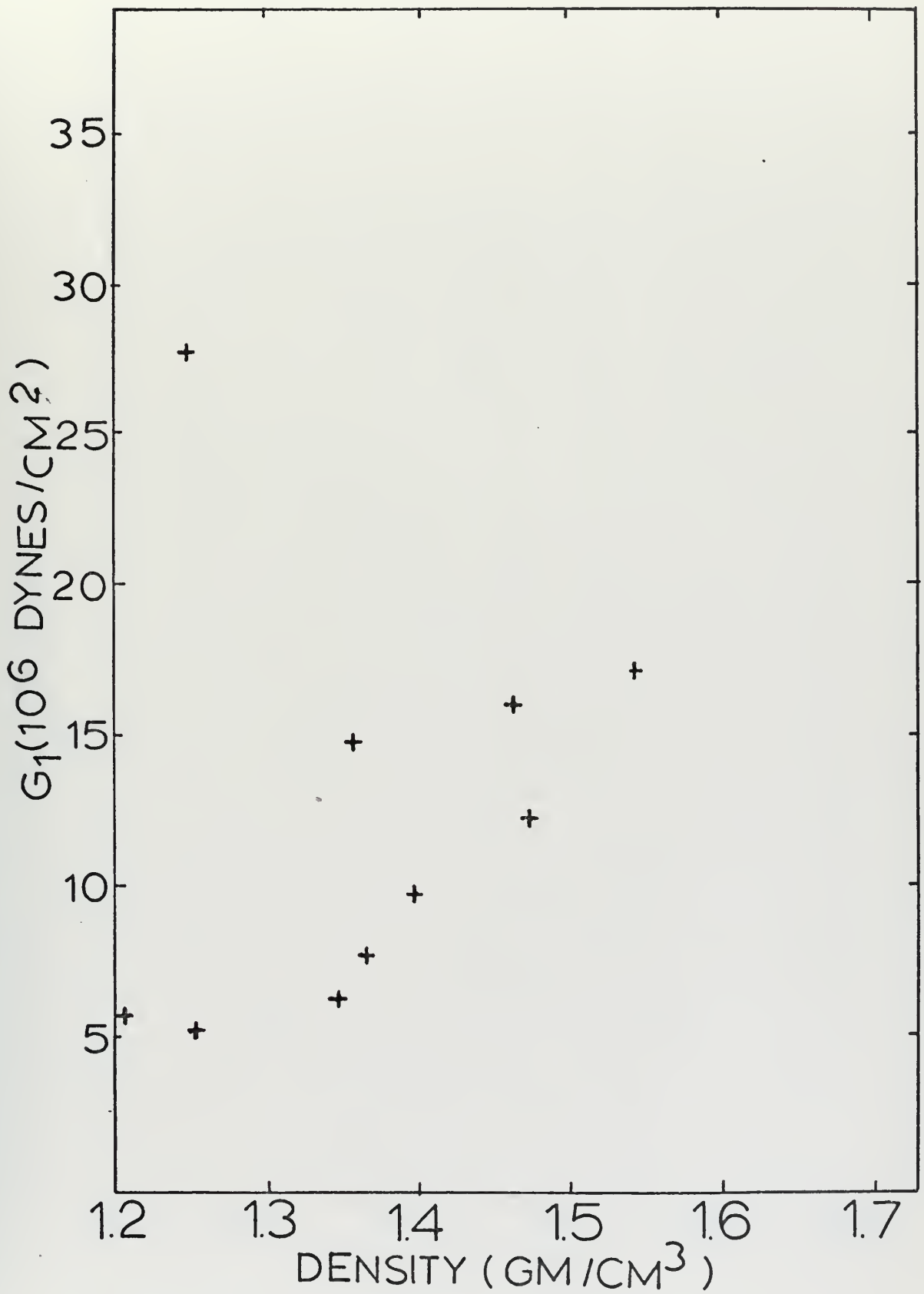


Figure 5. G₁ as a Function of Density

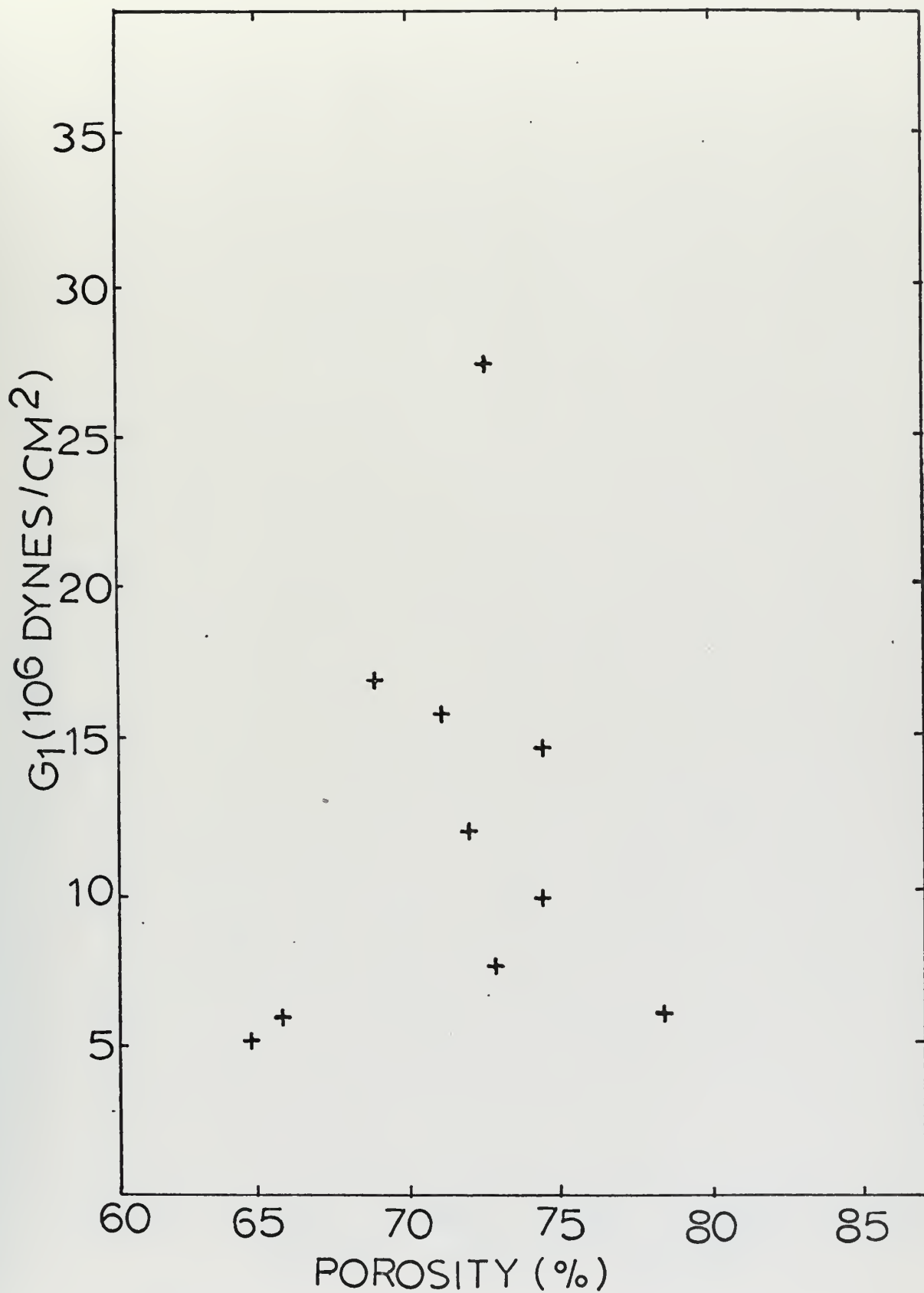


Figure 6. G_1 as a Function of Porosity

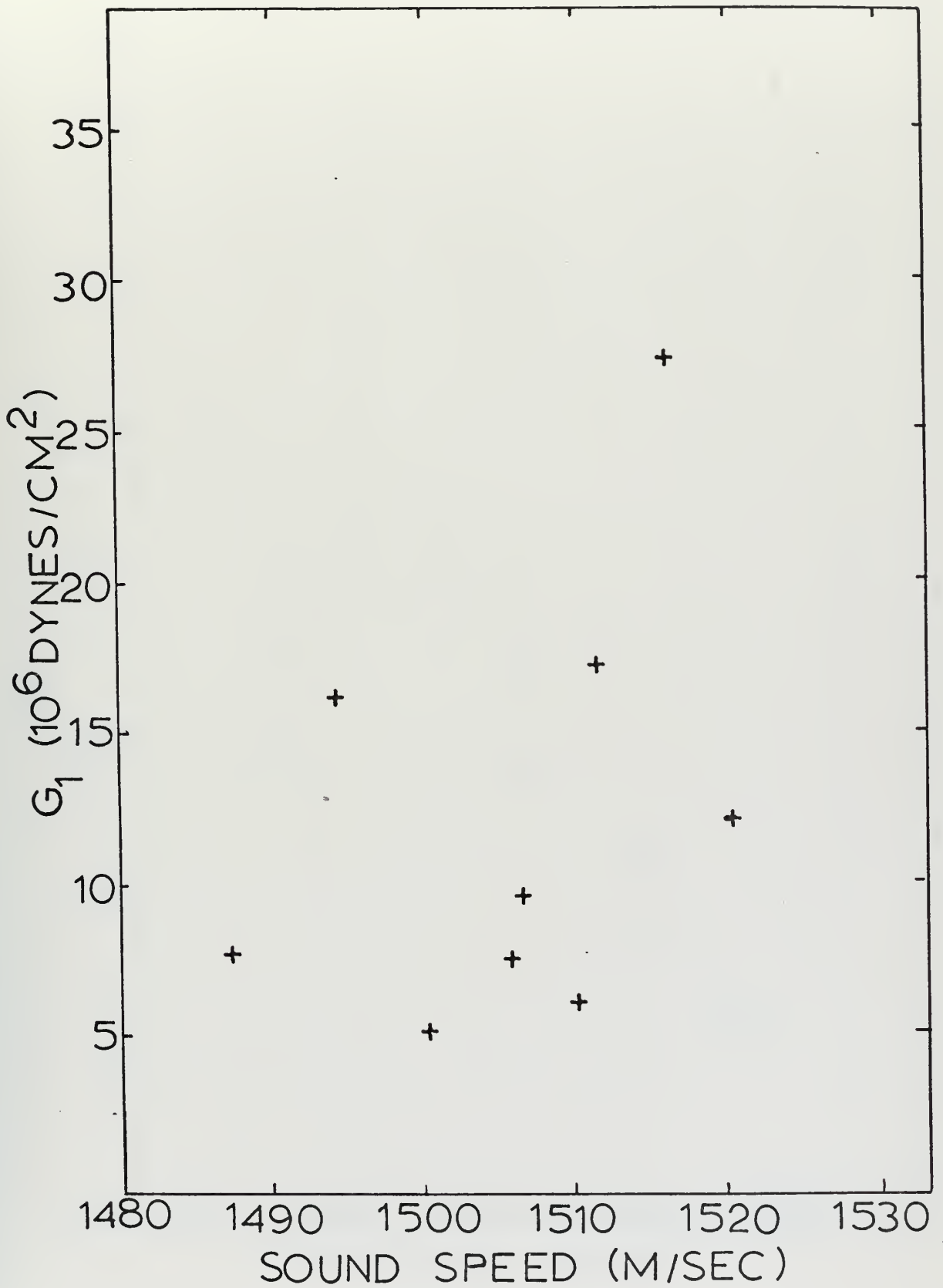


Figure 7. G_1 as a Function of Sound Speed

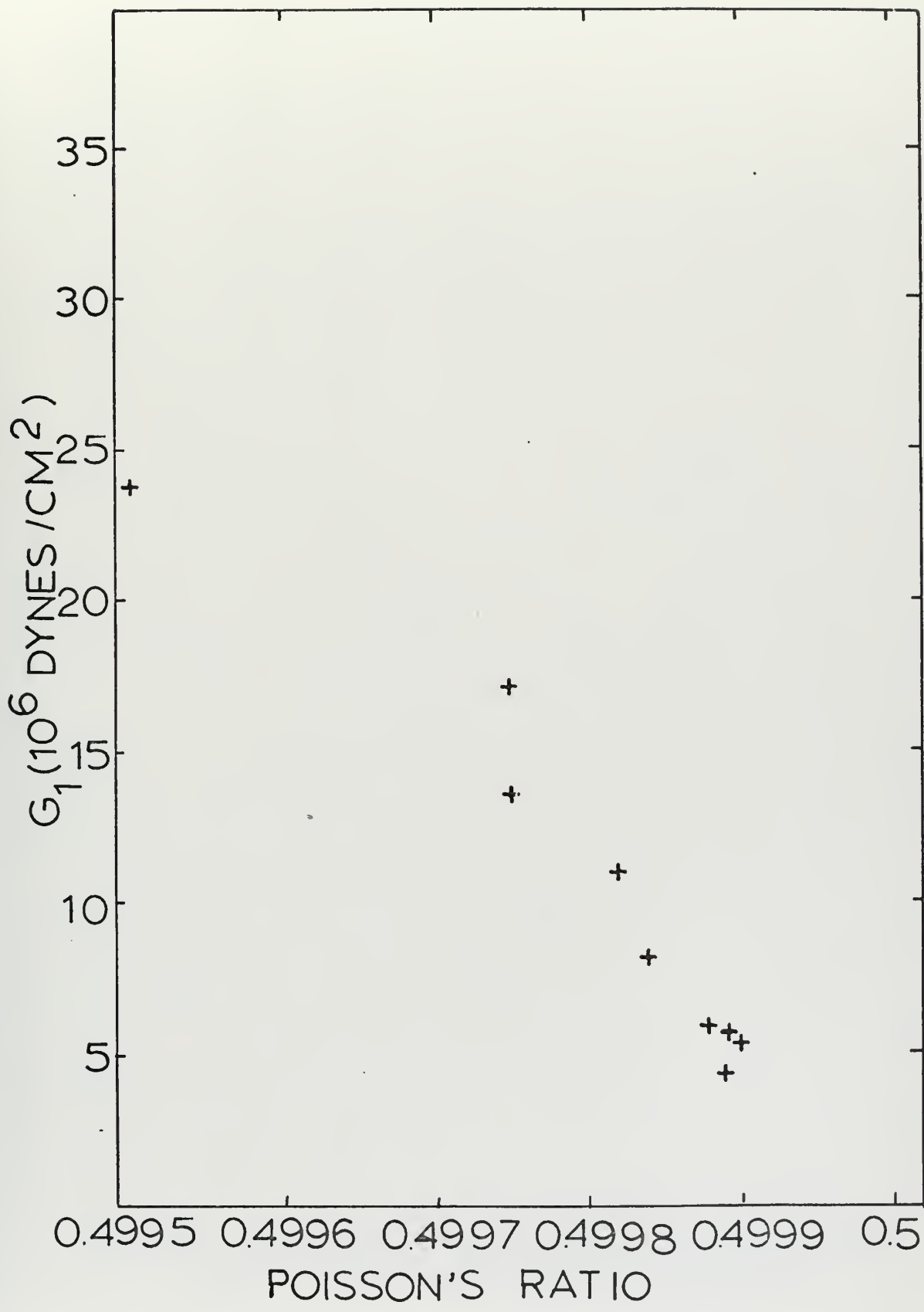


Figure 8. G_1 as a Function of Poisson's Ratio

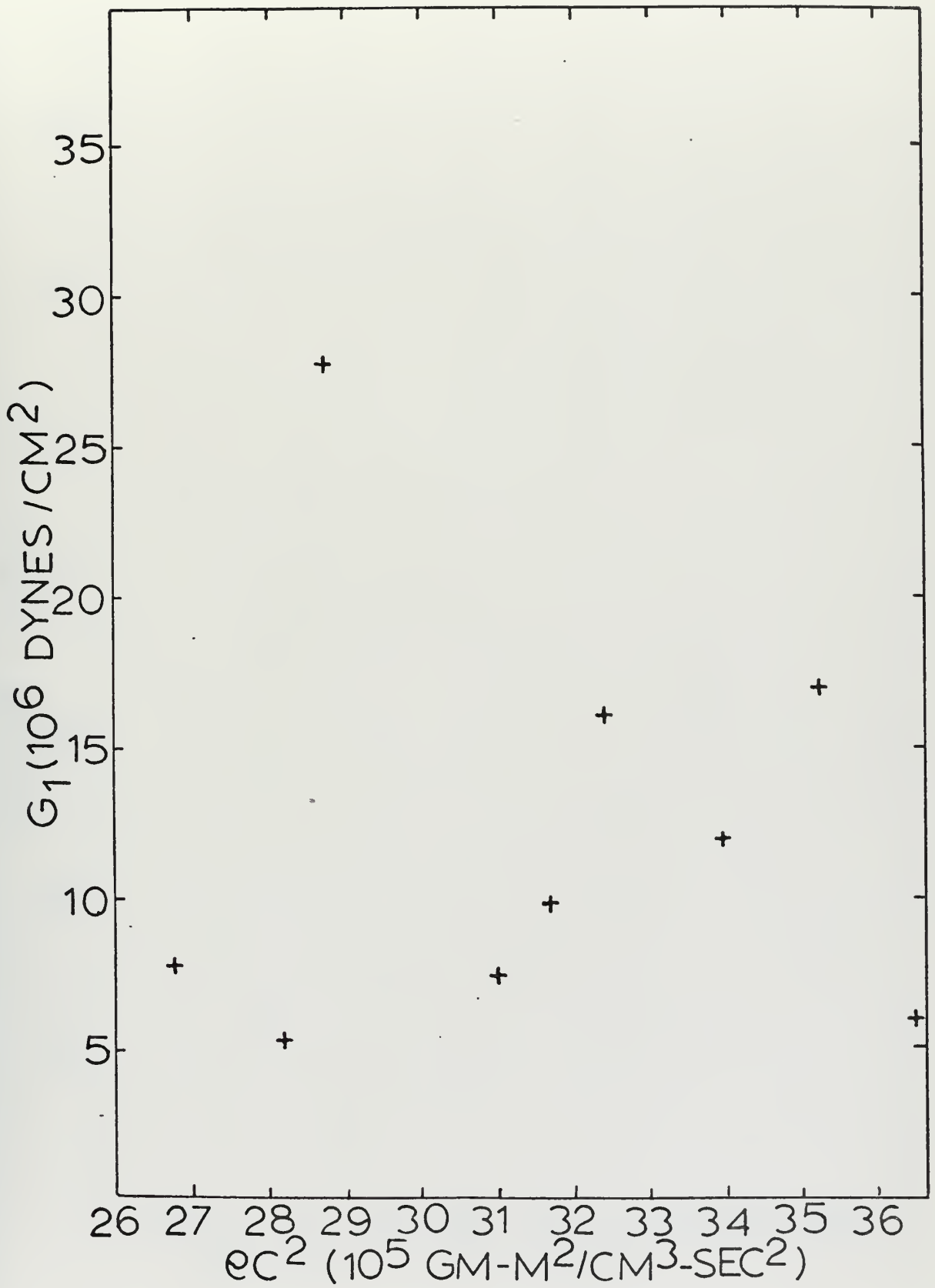


Figure 9. G_1 as a Function of Density and Sound Speed Squared

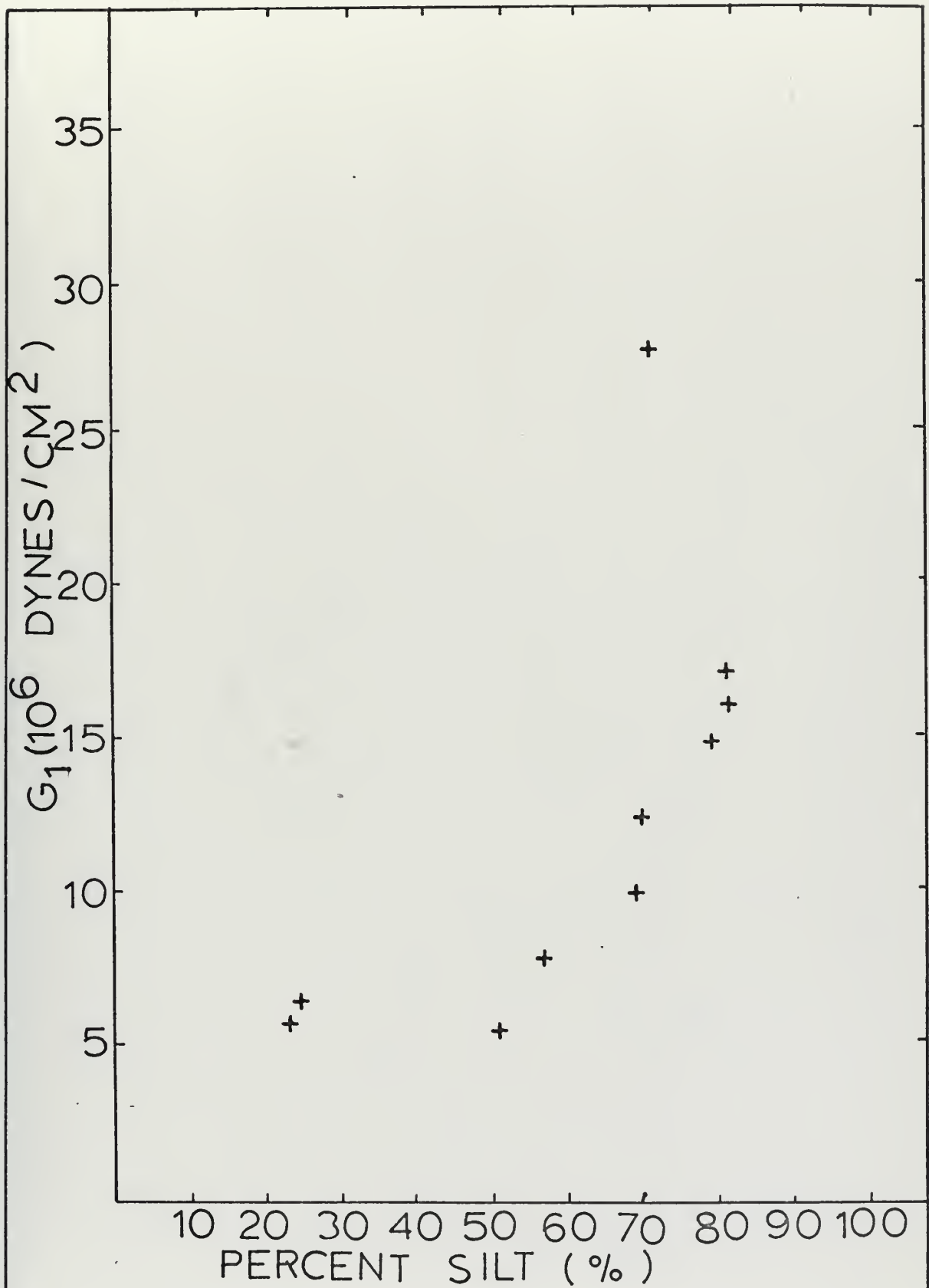


Figure 10. G_1 as a Function of Percent Silt

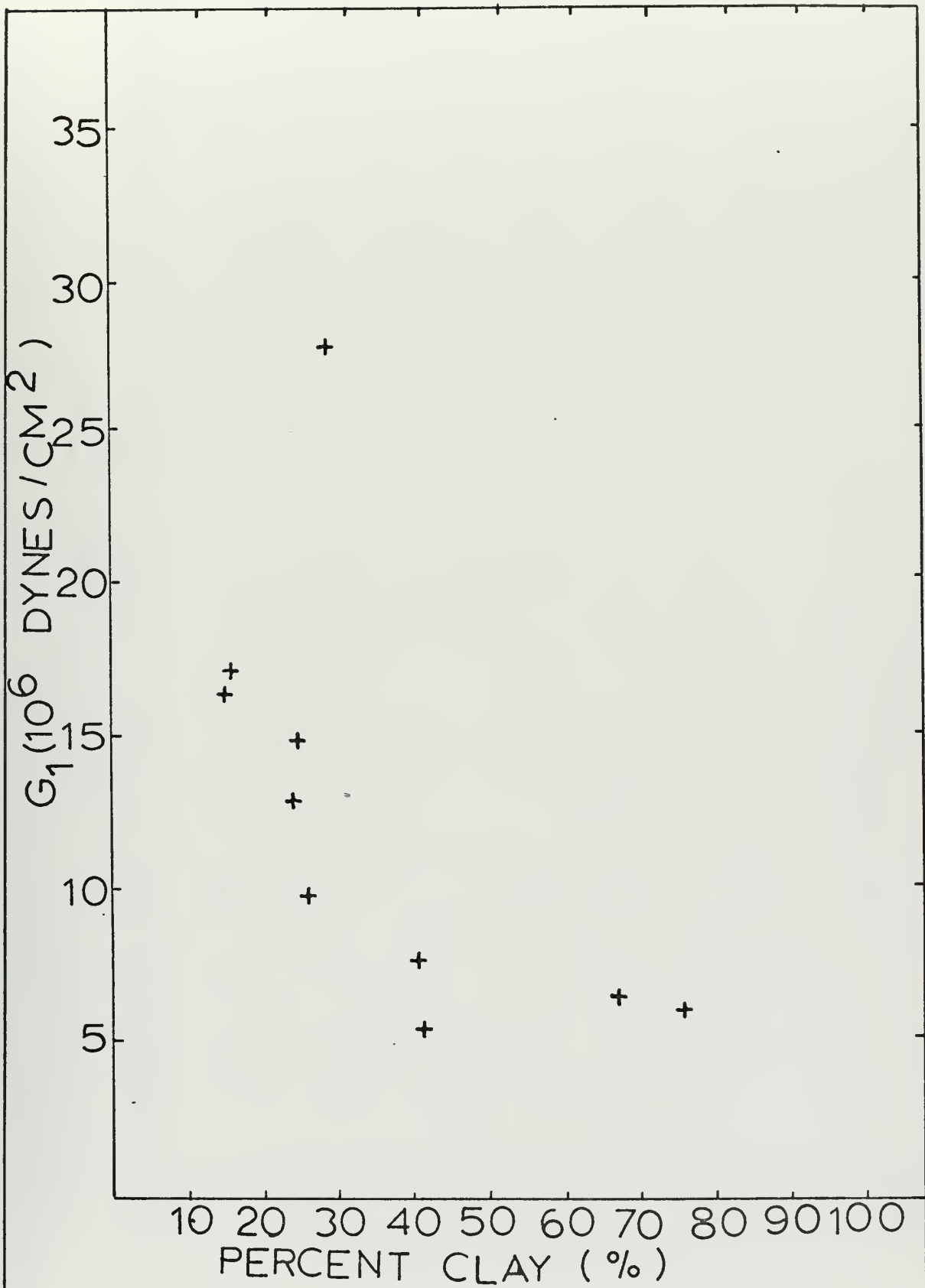


Figure 11. G_1 as a Function of Percent Clay

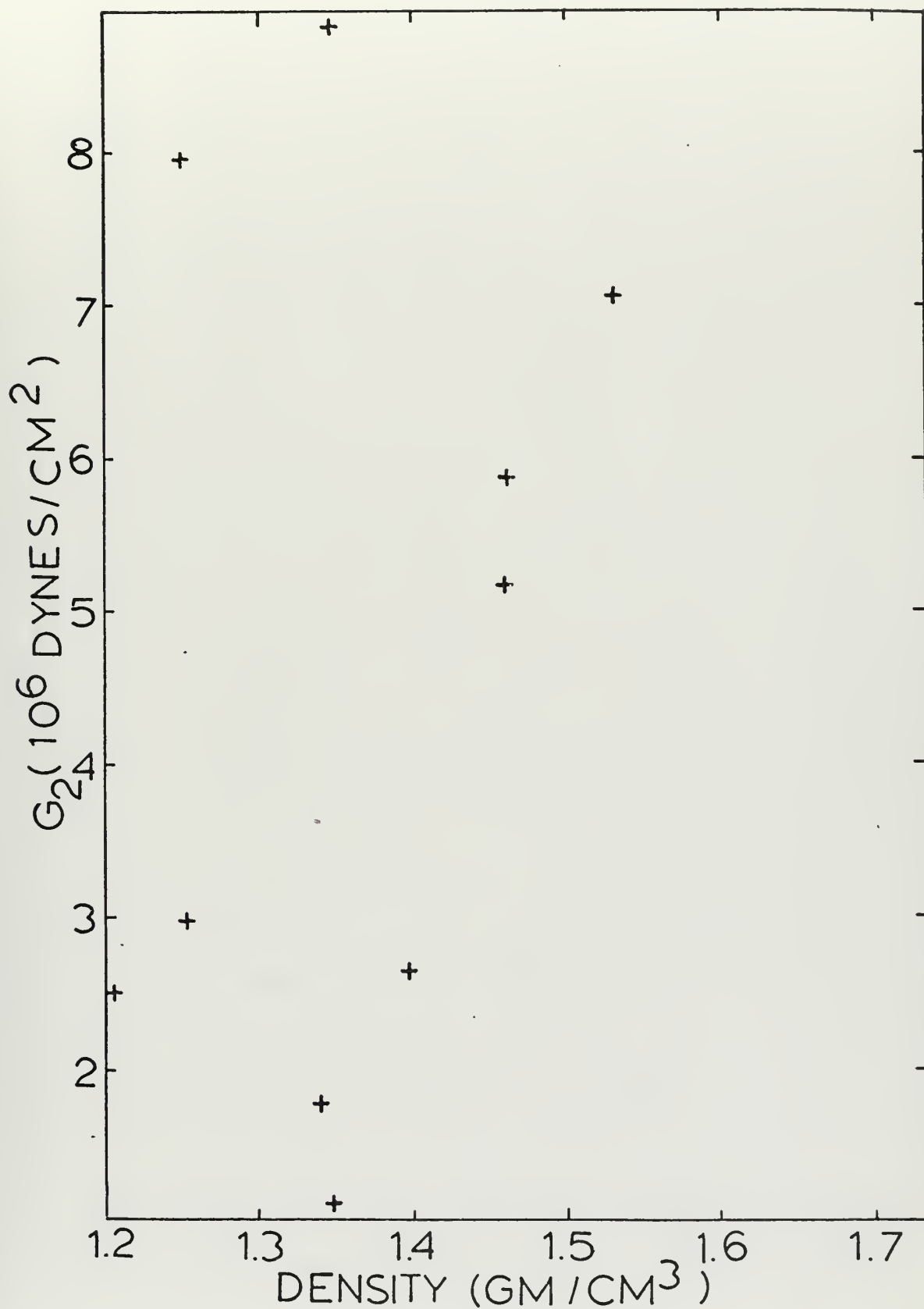


Figure 12. G₂ as a Function of Density

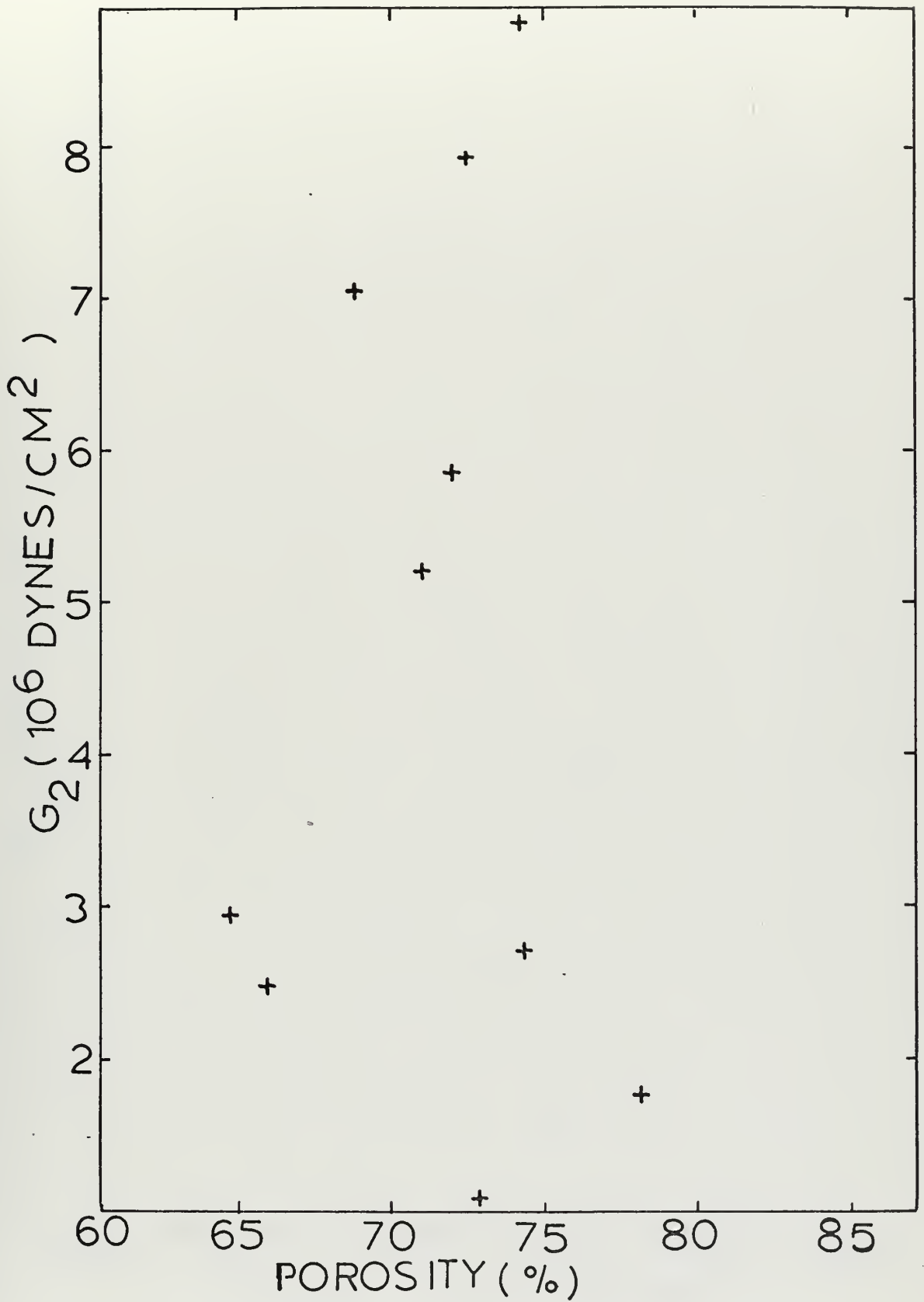


Figure 13. G_2 as a Function of Porosity

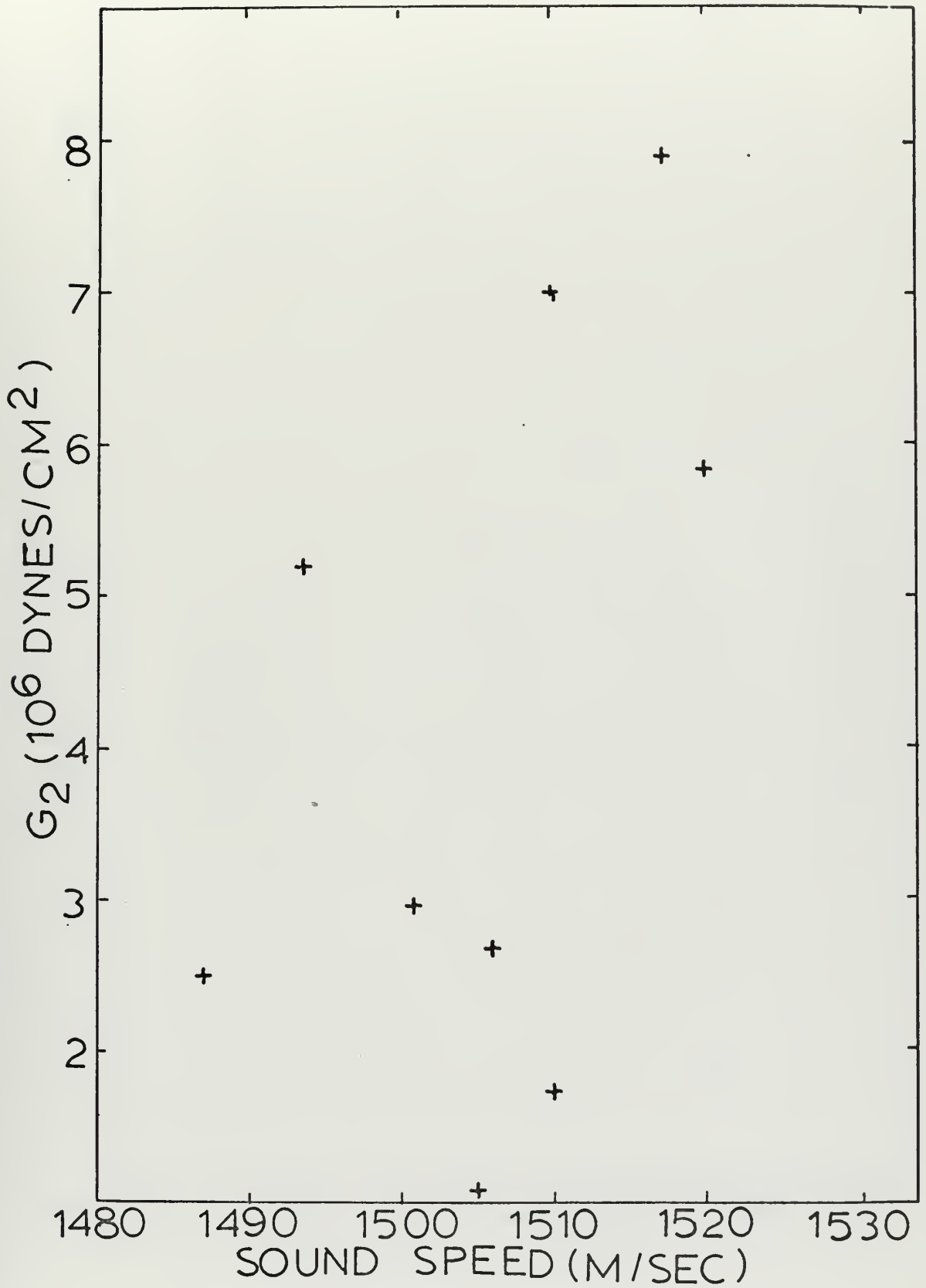


Figure 14. G₂ as a Function of Sound Speed

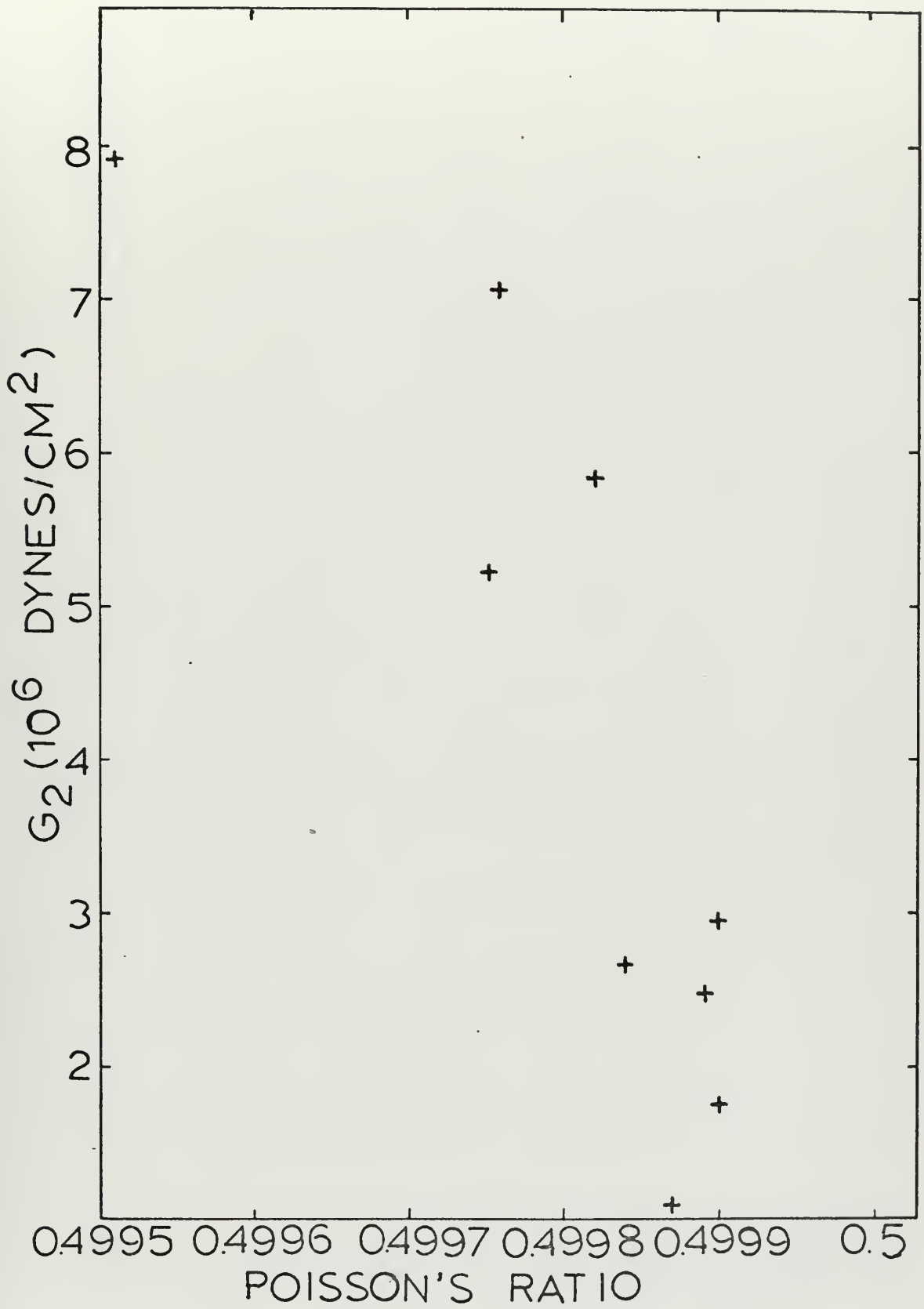


Figure 15. G_2 as a Function of Poisson's Ratio

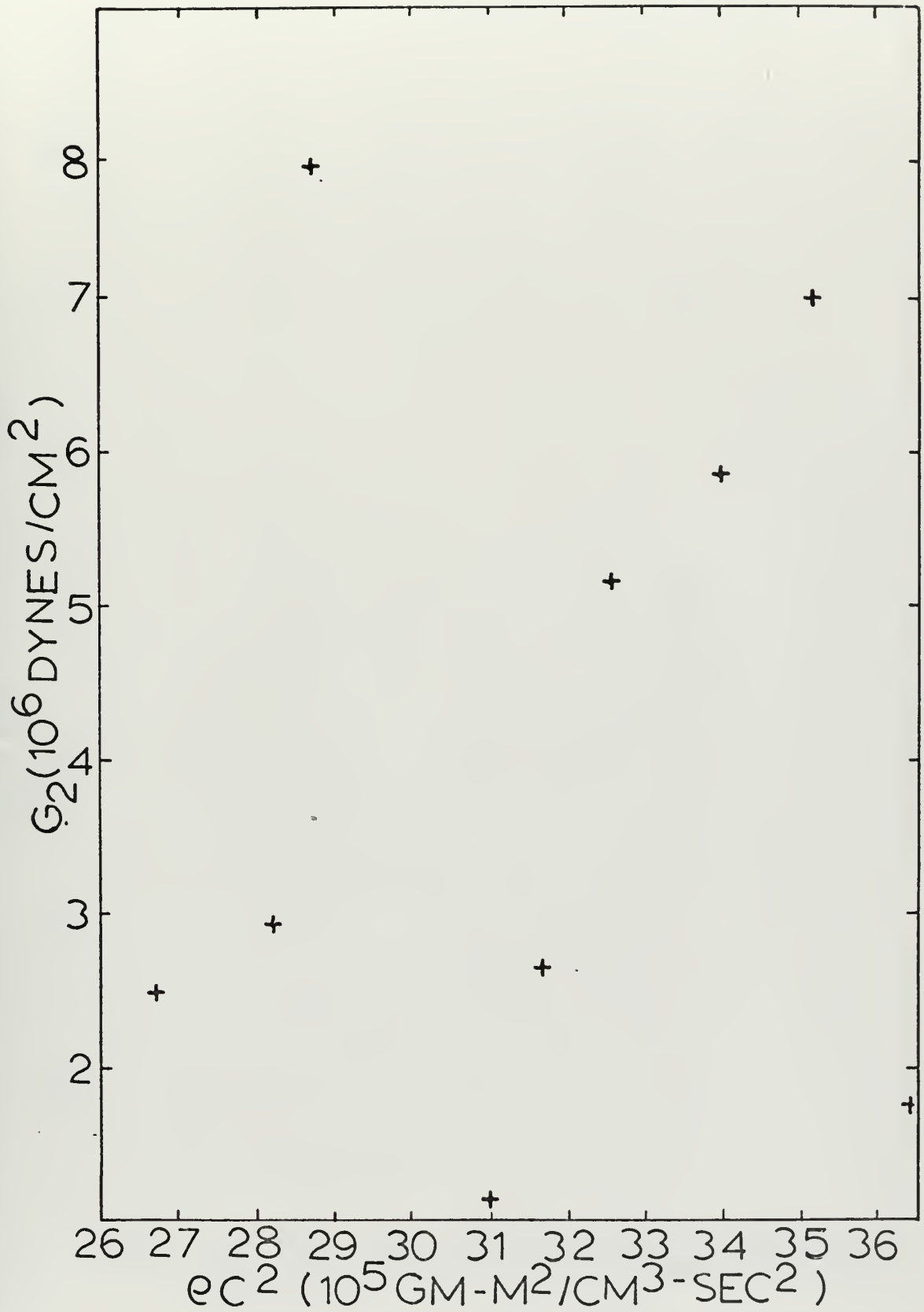


Figure 16. G_2 as a Function of Density and Sound Speed Squared

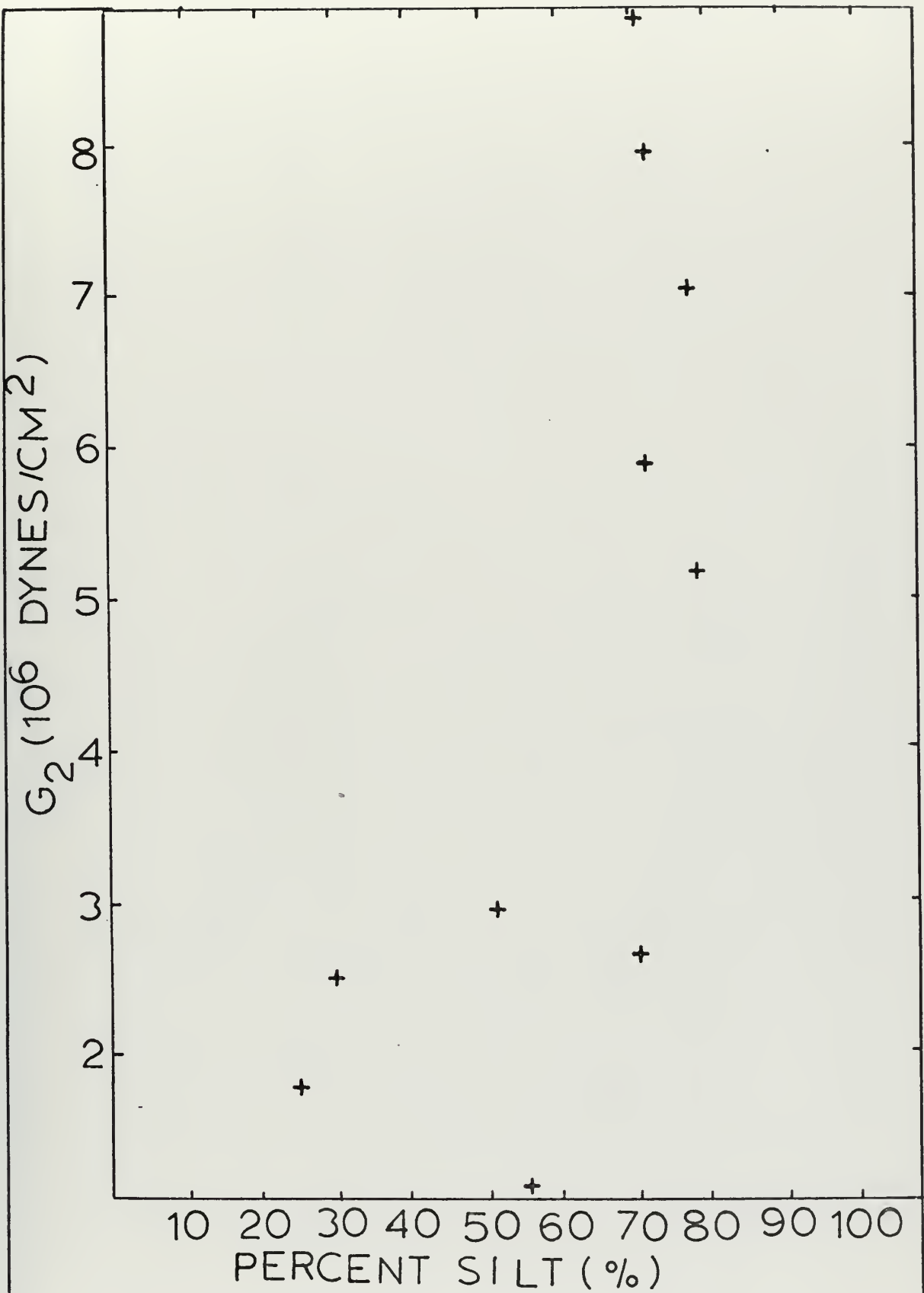


Figure 17. G_2 as a Function of Percent Silt

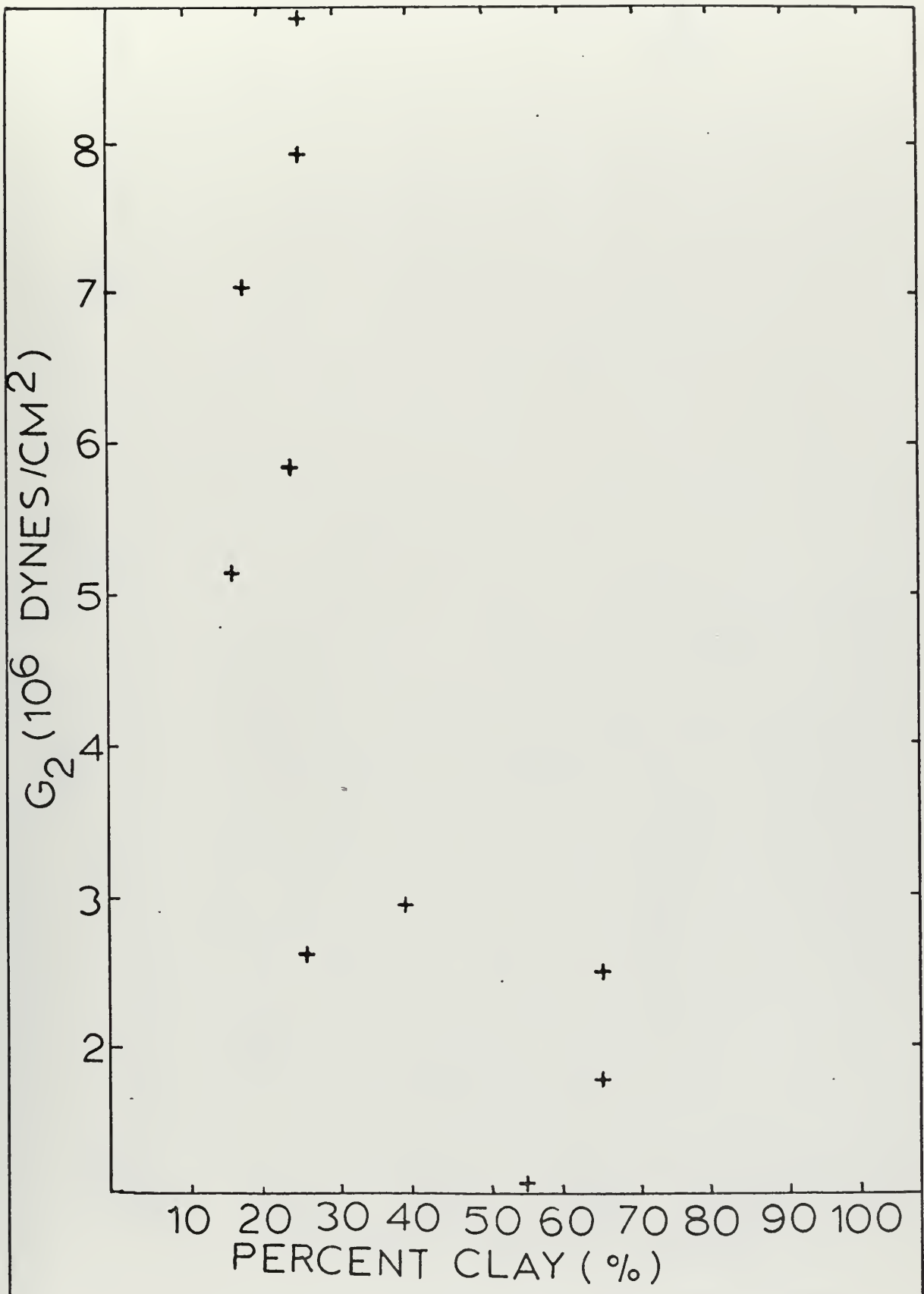


Figure 18. G_2 as a Function of Percent Clay

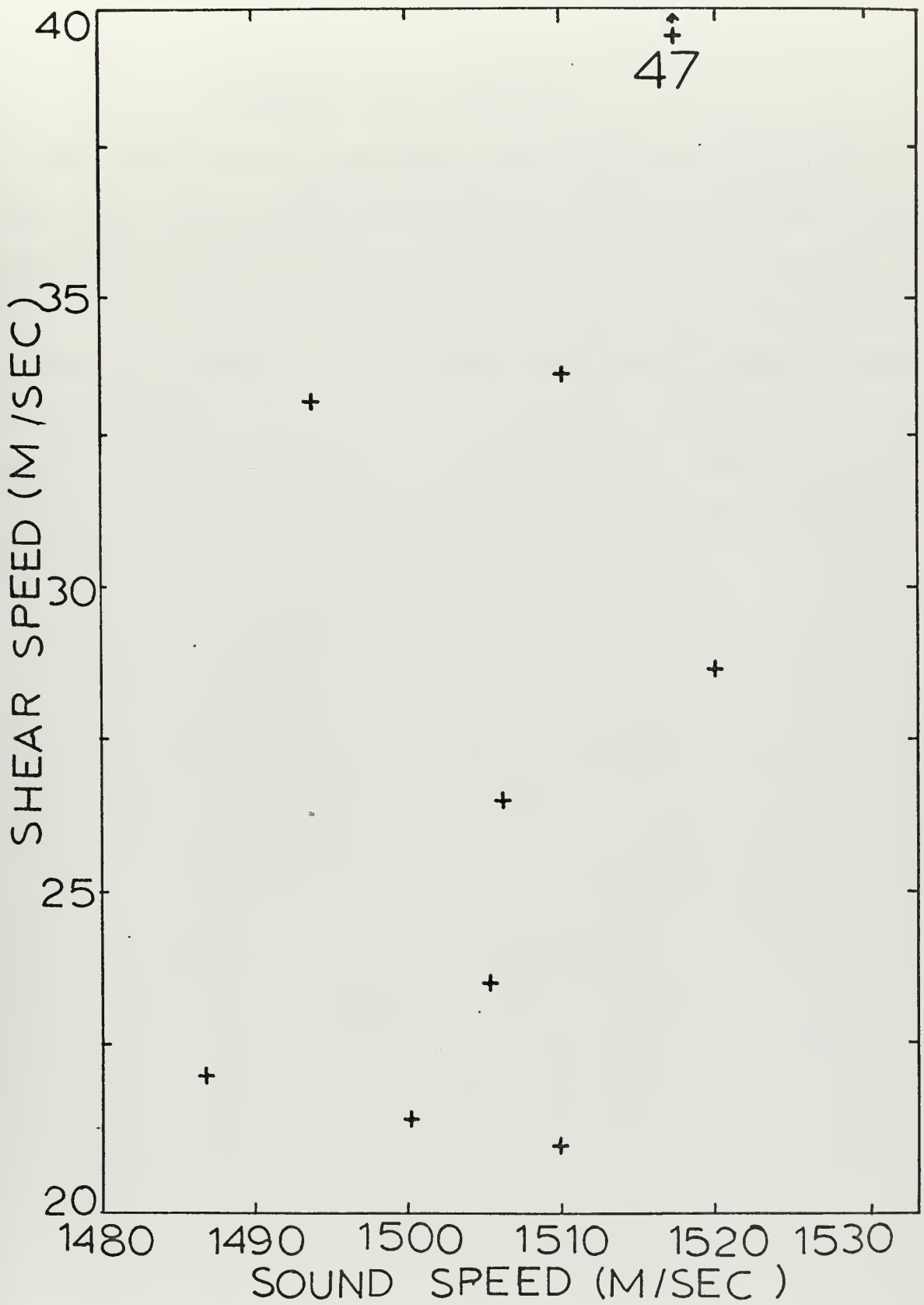


Figure 19. Shear Speed as a Function of Sound Speed

APPENDIX: CLAY MINERALOGY

The results of the quantitative analyses of the clay minerals from X-ray diffraction are shown in Table IV. The relatively high percentage of chlorite in these samples is due to river drainage from areas of outcrops of the Franciscan Formation. The graphs of G_1 and G_2 as a function of the various clay minerals show the data from this report as well as those from Bieda (1970)(Figures 20 - 25). Little in the way of definite trends may be seen, possibly due to the fact that these data are all from nearshore sediment samples.

TABLE IV. Clay Mineralogy

<u>SAMPLE</u>	<u>PERCENT MONTMORILLONITE</u>	<u>PERCENT ILLITE</u>	<u>PERCENT KAOLINITE</u>	<u>PERCENT CHLORITE</u>
2.	72.88	13.56	6.51	6.98
3.	69.31	13.97	8.05	8.66
4.	60.72	17.86	11.82	9.60
5.	51.35	21.62	12.16	14.86
6.	47.33	25.95	11.76	14.96
8.	64.91	12.21	10.53	12.37
9.	48.82	24.24	12.53	14.41

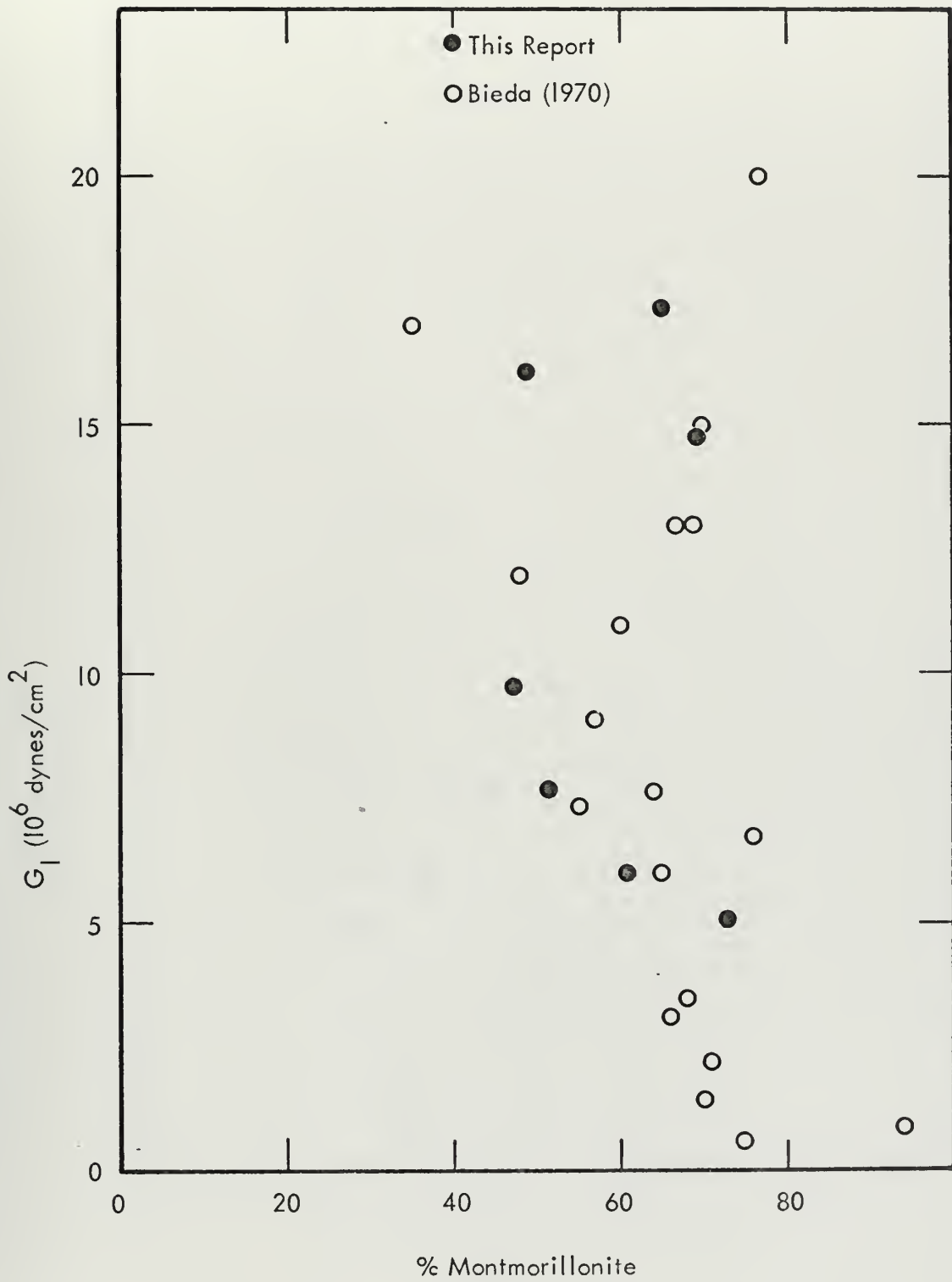


Figure 20. G_1 as a Function of Percent Montmorillonite

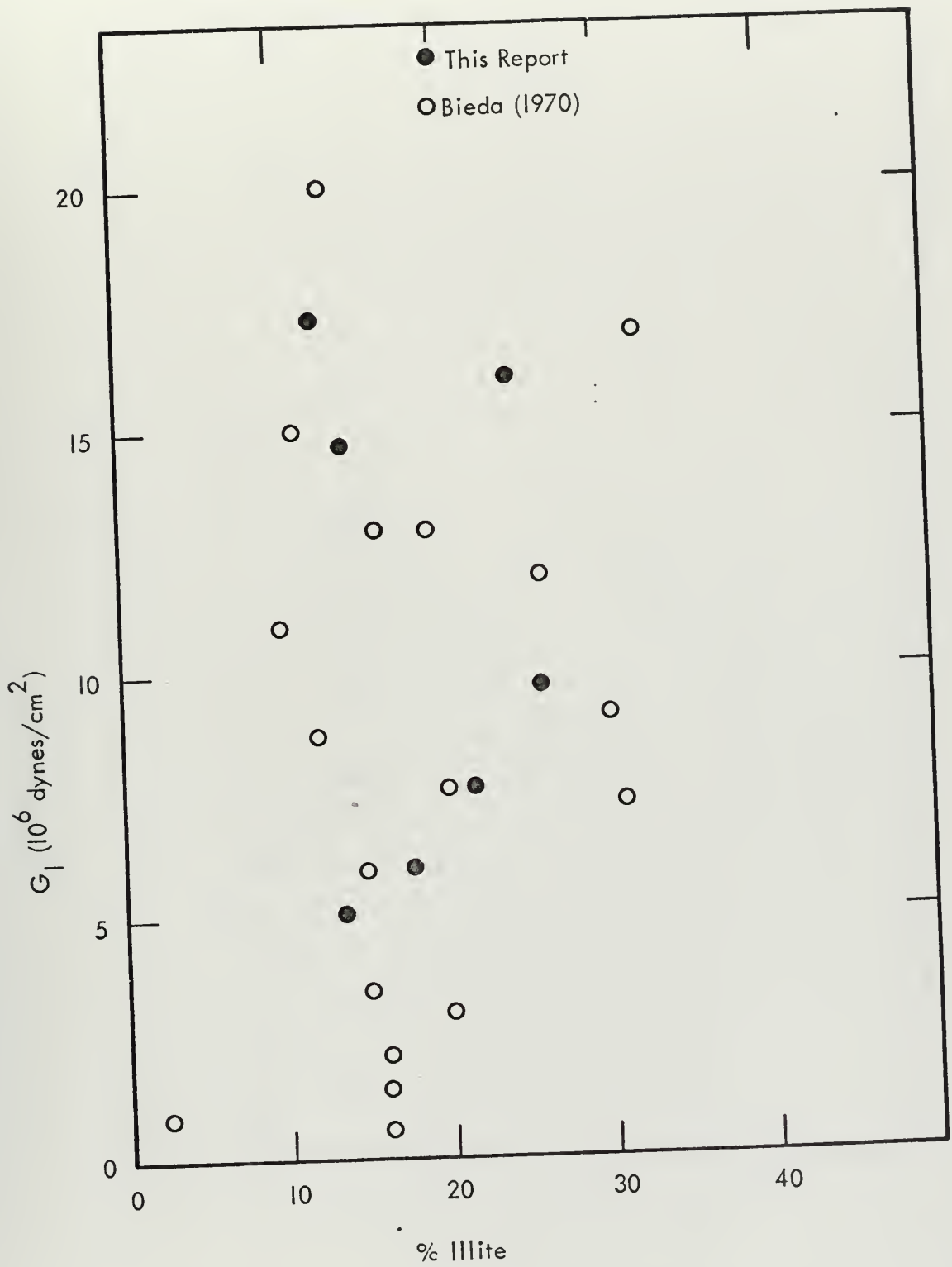


Figure 21. G_1 as a Function of Percent Illite

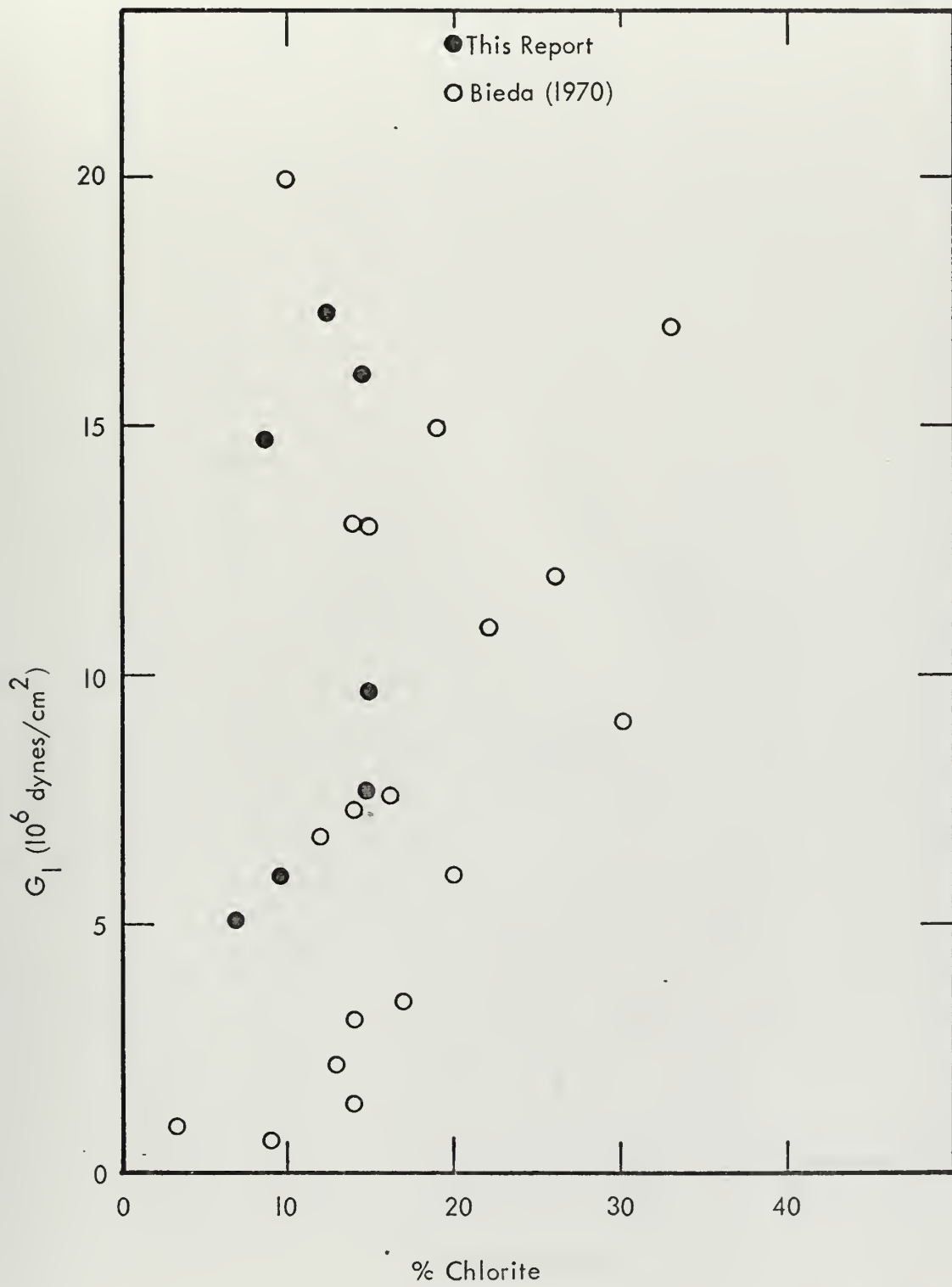


Figure 22. G_1 as a Function of Percent Chlorite

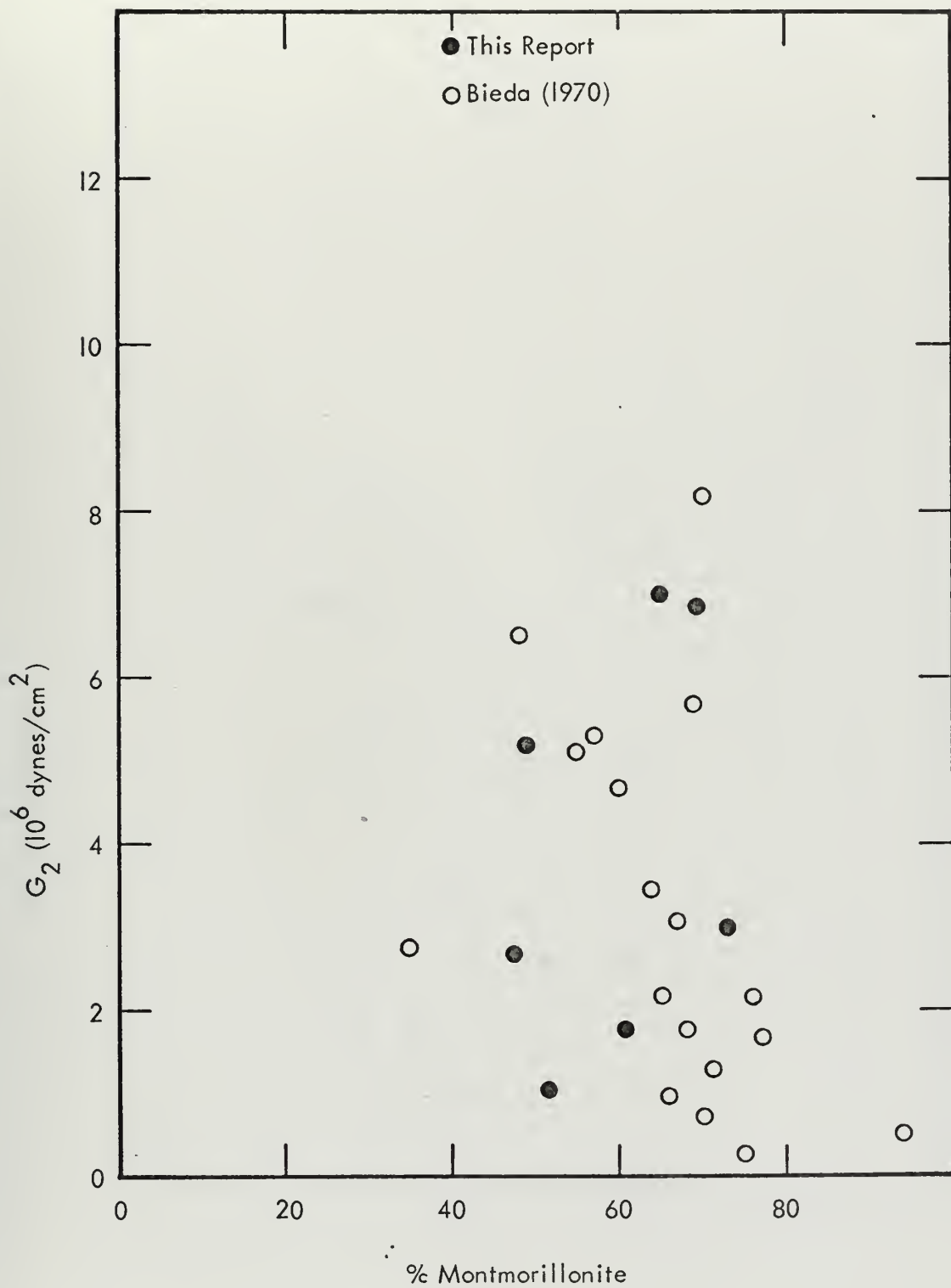


Figure 23. G_2 as a Function of Percent Montmorillonite

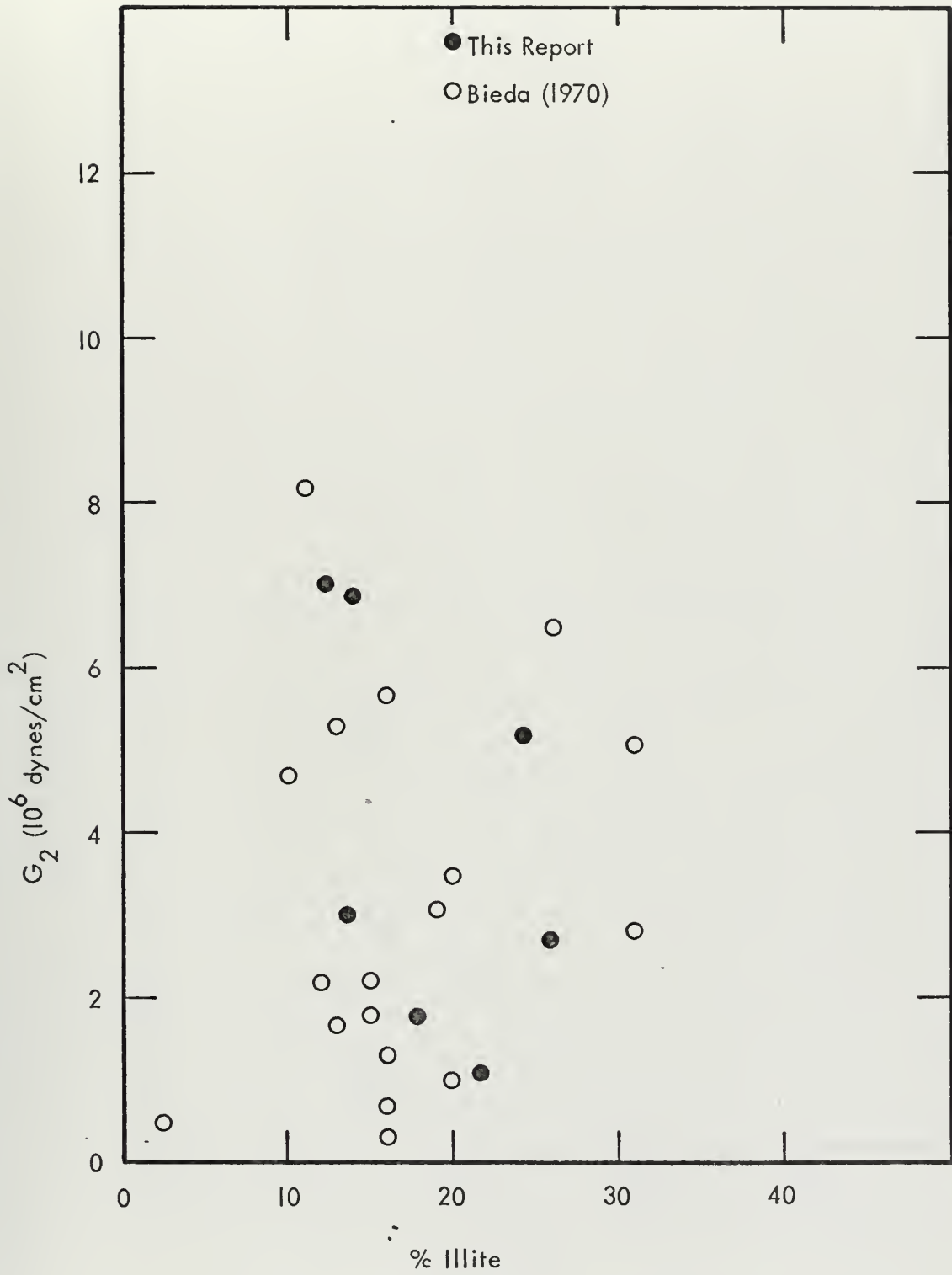


Figure 24. G_2 as a Function of Percent Illite

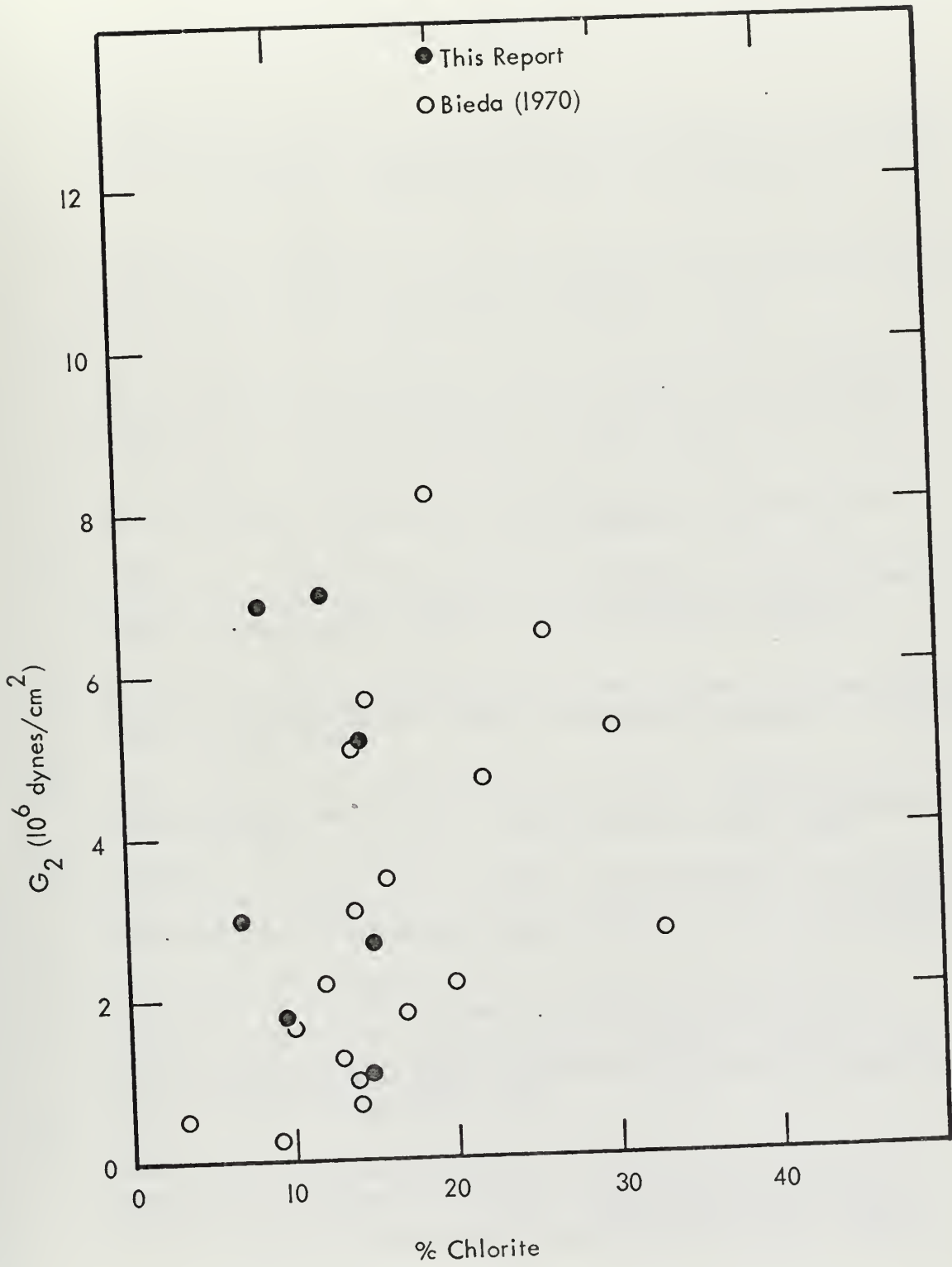


Figure 25. G_2 as a Function of Percent Chlorite

BIBLIOGRAPHY

1. Anderson, R.S., and G.V. Latham, Determination of Sediment Properties from First Shear Mode Rayleigh Waves Recorded on the Ocean Bottom, Journal of Geophysical Research, v. 74, No. 10, 1969, pp. 2747-2757.
2. Bieda, G.E., Measurement of the Viscoelastic and Related Mass Physical Properties of Some Continental Terrace Sediments, M.S. Thesis, Naval Postgraduate School, 1970.
3. Bucker, H.P., J.A. Whitney, G.S. Yee and R.R. Gardner, Reflection of Low-Frequency Sonar Signals from a Smooth Ocean Bottom, The Journal of the Acoustical Society of America, v. 31, No. 6, 1965, pp. 1037-1051.
4. Cagniard, L., Reflection and Refraction of Progressive Seismic Waves, McGraw-Hill Book Company, Inc., 1962.
5. Cohen, S.R., Measurement of the Viscoelastic Properties of Water Saturated Clay Sediments, M.S. Thesis, Naval Postgraduate School, 1968.
6. Davies, D., Dispersed Stoneley Waves on the Ocean Bottom, The Bulletin of the Seismological Society of America, v. 55, No. 5, 1965, pp. 903-918.
7. Ewing, W.M., W.S. Jardetzky and F. Press, Elastic Waves in Layered Media, McGraw-Hill Book Company, Inc., 1957.
8. Gallagher, J.J., and V.A. Nacce, Investigations of Sediment Properties in Sonar Bottom Reflectivity Studies, Underwater Sound Laboratory Report No. 944, 1968.
9. Hamilton, E.L., Sound Velocity, Elasticity and Related Properties of Marine Sediments, North Pacific, Part I: Sediment Properties, Environmental Control, and Empirical Relationships, Naval Undersea Research and Development Center Technical Report No. 143, 1969.
10. Hamilton, E.L., Sound Velocity, Elasticity and Related Properties of Marine Sediments, North Pacific, Part II: Elasticity and Elastic Constants, Naval Undersea Research and Development Center Technical Report No. 144, 1969.

11. Hamilton, E.L., H.P. Bucker, D.L. Keir, and J.A. Whitney, In Situ Determinations of the Velocities of Compressional and Shear Waves in Marine Sediments from a Research Submersible, Naval Undersea Research and Development Center Technical Report No. 163, 1969.
12. Hutchins, J.R., Investigations of the Viscoelastic Properties of a Water Saturated Sediment, M.S. Thesis, Naval Postgraduate School, 1967.
13. Kinsler, L.E., and A.R. Frey, Fundamentals of Acoustics, 2nd Edition, Wiley and Sons, Inc., 1962.
14. Mason, W.P., Measurements of the Viscosity and Shear Elasticity of Liquids by Means of a Torsionally Vibrating Crystal, Transactions of the A.S.M.E., May 1947, pp. 359-370.
15. McSkimin, H.J., Measurements of Dynamic Shear Viscosity and Stiffness of Viscous Liquids by Means of Traveling Torsional Waves, The Journal of the Acoustical Society of America, v. 24, No. 4, 1952, pp. 355-365.
16. Scholte, J.G., On the Large Displacements Commonly Regarded as Caused by Love-Waves and Similar Dispersive Surface-Waves, Nederlandse Akademie Van Wetenschappern, Proceedings, v. 51, pp. 533-543, 642-649, 828-835, 969-976.
17. Stoneley, M.A., Elastic Waves at the Surface of Separation of Two Solids, Royal Society of London, Proceedings, v. 106A, 1924, pp. 416-428.
18. Strict, E., and A.S. Ginzburg, Stoneley-Wave Velocities for a Fluid-Solid Interface, Bulletin of the Seismological Society of America, v. 46, 1956, pp. 281-292.
19. Strict, E., W.L. Rover and T.F. Vining, Propagation of Elastic Wave Motion from an Impulsive Source Among a Fluid-Solid Interface, Proceedings of the Royal Society of London, 1959, pp. 455-523.
20. Tooley, R.D., T.W. Spencer and H.F. Sagoci, Reflection and Transmission of Plane Compressional Waves, Geophysics, v. 30, No. 4, August 1965.
21. Williard, G.W., Temperature Coefficient of Ultrasonic Velocity in Solutions, The Journal of the Acoustical Society of America, v. 19, No. 1, 1947, pp. 235-241.

INITIAL DISTRIBUTION LIST

	No. Copies
1. Defense Documentation Center Cameron Station Alexandria, Virginia 22314	2
2. Library, Code 0212 Naval Postgraduate School Monterey, California 93940	2
3. Dr. O.B. Wilson, Jr., (Code 61) Department of Physics Naval Postgraduate School Monterey, California 93940	5
4. Dr. R.S. Andrews (Code 58Ad) Department of Oceanography Naval Postgraduate School Monterey, California 93940	5
5. Dr. E.L. Hamilton Naval Undersea Research & Development Center San Diego, California 92132	1
6. Dr. William R. Bryant Texas A&M University Department of Oceanography College Station, Texas 77843	1
7. Dr. Davis A Fahlquist Texas A&M University Department of Geophysics College Station, Texas 77843	1
8. Mr. James J. Gallagher Oceanography Branch Ocean Sciences Division Naval Underwater Sound Laboratory New London, Connecticut 06320	1
9. Mr. Dave Kier Sound Propagation Branch Naval Undersea Research & Development Center San Diego, California 92132	1

10. LTJG George E. Bieda, USN 1
Naval Nuclear Power
Mare Island, Vallejo 94592

11. Lt James B. Lasswell, USN 1
c/o Col. A.B. Lasswell, USMC (Ret.)
Post Office Box 886
Rancho Santa Fe, California 92067

12. Mr. Rockne S. Anderson 1
Acoustical Oceanography Division
US Naval Oceanographic Office
Washington, D.C. 20390

13. Dr. H.P. Bucker 1
Naval Research Laboratory
Washington, D.C. 20390

DOCUMENT CONTROL DATA - R & D

(Security classification of title, body of abstract and indexing annotation must be entered when the overall report is classified)

1. ORIGINATING ACTIVITY (Corporate author) Naval Postgraduate School Monterey, California 93940		2a. REPORT SECURITY CLASSIFICATION Unclassified	
		2b. GROUP	
3. REPORT TITLE A Comparison of Two Methods for Measuring Rigidity of Saturated Marine Sediments			
4. DESCRIPTIVE NOTES (Type of report and, inclusive dates) Master's Thesis; December 1970			
5. AUTHOR(S) (First name, middle initial, last name) James Bryan Lasswell			
6. REPORT DATE December 1970	7a. TOTAL NO. OF PAGES 65	7b. NO. OF REFS 21	
8a. CONTRACT OR GRANT NO.	9a. ORIGINATOR'S REPORT NUMBER(S)		
b. PROJECT NO.			
c.	9b. OTHER REPORT NO(S) (Any other numbers that may be assigned this report)		
d.			
10. DISTRIBUTION STATEMENT This document has been approved for public release and sale; its distribution is unlimited			
11. SUPPLEMENTARY NOTES		12. SPONSORING MILITARY ACTIVITY Naval Postgraduate School Monterey, California 93940	
13. ABSTRACT The results of two different methods for determining the rigidity modulus of a soft sediment are compared. In one method the resonant characteristics of a torsionally oscillating rod which are sensitive to the shear acoustic impedance of the sediment in which the rod is imbedded determine the complex rigidity. The second method utilizes the observation of the phase velocity of an interface wave at the water-sediment boundary. Shear wave speeds computed from the experimental data from both methods are quite similar in magnitude. For the sediment used here, the average value of shear wave speed determined from the interface wave experiment was 33 m/sec while the shear wave speed determined from the measured rigidity was 29 m/sec. The difference lies within experimental uncertainty. Trends in the mass-physical properties of the sediments are investigated by comparing graphically the dependence of both the real and imaginary parts of the complex rigidity on density, porosity, sound speed, silt and clay percentages, Poisson's ratio and density times sound speed squared.			

14 KEY WORDS	LINK A		LINK B		LINK C	
	ROLE	WT	ROLE	WT	ROLE	WT
Viscoelastic						
Shear Modulus						
Rigidity						
Shear Speed						
Stoneley Wave						
Interface Wave						
Resonant						
Sediment						

5 JUN 72

21585

Thesis

126119

L275 Lasswell

c.1 A comparison of two
methods for measuring
rigidity of saturated
marine sediments.

5 JUN 72

21585

5 JUN 72

21585

Thesis

126119

L275 Lasswell

c.1 A comparison of two
methods for measuring
rigidity of saturated
marine sediments.

thesL275

A comparison of two methods for measurin



3 2768 002 12283 0

DUDLEY KNOX LIBRARY